



**HAL**  
open science

## Control of Thrust-Propelled Underactuated Vehicles

Minh Duc Hua, Tarek Hamel, Pascal Morin, Claude Samson

► **To cite this version:**

Minh Duc Hua, Tarek Hamel, Pascal Morin, Claude Samson. Control of Thrust-Propelled Underactuated Vehicles. [Research Report] RR-6453, INRIA. 2008, pp.42. inria-00258092v2

**HAL Id: inria-00258092**

**<https://inria.hal.science/inria-00258092v2>**

Submitted on 28 Feb 2008

**HAL** is a multi-disciplinary open access archive for the deposit and dissemination of scientific research documents, whether they are published or not. The documents may come from teaching and research institutions in France or abroad, or from public or private research centers.

L'archive ouverte pluridisciplinaire **HAL**, est destinée au dépôt et à la diffusion de documents scientifiques de niveau recherche, publiés ou non, émanant des établissements d'enseignement et de recherche français ou étrangers, des laboratoires publics ou privés.

# *Control of Thrust-Propelled Underactuated Vehicles*

Minh-Duc HUA — Tarek HAMEL — Pascal MORIN — Claude SAMSON

**N° 6453**

February 2008

Thème NUM



*Rapport  
de recherche*



## Control of Thrust-Propelled Underactuated Vehicles

Minh-Duc HUA \* , Tarek HAMEL † , Pascal MORIN \* , Claude SAMSON \*

Thème NUM — Systèmes numériques  
Projets AROBAS

Rapport de recherche n° 6453 — February 2008 — 42 pages

**Abstract:** The basics of a control framework for a class of underactuated vehicles immersed in an ambient fluid with the objective of stabilizing reference trajectories are developed. These vehicles are characterized by their means of propulsion which essentially relies on the production of a thrust force along a single body-fixed direction, with the complement of full torque actuation for attitude control (i.e. a typical actuation structure for aircrafts, VTOL vehicles, submarines, etc.). Interactions with the surrounding fluid are difficult to model precisely and the source of possibly strong perturbations. They constitute a major issue for stable motion control of these systems. Novel nonlinear feedback control laws are proposed to compensate for modeling errors and perform robustly against such perturbations. Simulation results illustrating these properties on a VTOL vehicle submitted to wind gusts are presented.

**Key-words:** underactuated vehicle, nonlinear control, velocity stabilization, trajectory tracking, bounded nonlinear integrator, dissipativity.

\* Minh Duc Hua, Pascal Morin, and Claude Samson are with INRIA, 2004 Route des Lucioles, 06902 Sophia Antipolis, France. E-mails: *Minh\_Duc.Hua@inria.fr*, *Pascal.Morin@inria.fr*, *Claude.Samson@inria.fr*

† Tarek Hamel is with I3S-CRNS, Les Algorithmes, Bat. Euclide B, 2000 Route des Lucioles, BP.121, 06903 Sophia Antipolis, France. E-mail: *thamel@i3s.unice.fr*

## Commande d'une classe de véhicules sous-actionnés

**Résumé :** Cet article établit les bases d'une approche générale de commande pour une classe de véhicules sous-actionnés immergés dans un fluide (air, eau, etc.), dans le but de stabiliser des trajectoires de référence en attitude, en vitesse linéaire, ou en position. Ces véhicules sont caractérisés par leur moyen de propulsion qui consiste en une force de poussée le long d'une direction fixe liée au véhicule, et un actionnement complet au niveau des couples pour le contrôle d'attitude. Il s'agit d'une structure d'actionnement typique pour des avions, des véhicules de type VTOL (Vertical Take-Off and Landing), des sous-marins, etc. Les interactions avec le fluide environnant sont difficiles à modéliser et/ou mesurer précisément, et sont la source de perturbations qui peuvent être importantes. Elles constituent un problème majeur pour la stabilité de ces systèmes. De nouvelles lois de commande par retour d'état non-linéaires sont ici proposées afin de compenser les erreurs de modélisation et assurer un comportement robuste face aux perturbations. Ces propriétés sont illustrées par des résultats de simulation portant sur un modèle de véhicule de type VTOL.

**Mots-clés :** véhicule sous-actionné, control non-linéaire, stabilisation de vitesse, poursuite de trajectoire, intégrateur non-linéaire borné, dissipativité.

## 1 Introduction

Airplanes, helicopters and other Vertical Take-Off and Landing (VTOL) vehicles, blimps, rockets, hydroplanes, ships, submarines are generally *underactuated*. These vehicles are basically composed of a main body immersed in a fluid medium (air or water), and they are commonly controlled via i) a propulsive thrust force directed along a body-fixed privileged axis, and ii) a torque vector with one, two or three complementary independent components in charge of modifying the body's orientation. These vehicles are underactuated in the sense that, apart from the direction associated with the thrust force, the other possible direction(s) of displacement is (are) not directly actuated. Interestingly, the above-mentioned structural similitude has seldom been systematically exploited to develop a general control framework for these vehicles. Various reasons can be proposed. For instance, there exist important differences between an airplane and a ship. The first vehicle evolves in air and 3D-space, whereas the other is (partly) immersed in water and essentially moves on a 2D-plane; the ambient fluid is not the same and it produces either aerodynamic or hydrodynamic reaction forces with different properties and magnitude; gravity is not compensated by buoyancy in the case of an airplane, but lift-force effects are more systematic and preponderant; mass-added effects mostly concern ships, submarines, and blimps; etc. Another probable reason is historical: aerospace and naval engineering communities involved in the control of these vehicles have not addressed common issues (the design of autopilots, for instance) in a coordinated manner, nor at the same time, nor with the same constraints (physical, economical, etc.), nor even with the same approaches. The present paper aims at developing a global approach for the control of this family of underactuated vehicles, knowing that the number of civilian and military applications involving various autonomous robotic vehicles is continuously growing.

Another important motivation of this work is related to robustness issues, which can be critical for these systems due to a combination of factors. First, the complexity of aero/hydro-dynamic effects impedes obtaining a precise dynamical model, valid in a large operating domain. Then, these vehicles are often subjected to perturbations (wind gusts, sea currents, etc.) which may be rapidly changing and whose magnitude can be commensurable with the available actuation power. Finally, measurement/estimation errors of the vehicle's pose can be significant. Of course, these issues have long been investigated for many types of vehicles in the context of linear control (see e.g. [1, 7, 8, 25] and the references therein). More generally, all kinds of linear control methods (pole placement,  $H_2$  and  $H_\infty$  optimization, LQR optimal control, etc.) have been applied to these systems. They concern Single-Input-Single-Output (SISO) Control Augmented Systems (CAS) associated with the regulation of a single variable (pitch, yaw, roll angle, altitude, longitudinal velocity, etc.) as well as Multi-Input-Multi-Output (MIMO) versions of these systems. However, they guarantee a limited domain of stability and are often based on restrictive assumptions (e.g. hovering regime without wind gusts for VTOL vehicles). For these reasons, nonlinear control design methods (feedback linearization, backstepping, sliding mode, etc.) have been increasingly investigated in recent studies [3, 12, 14, 17, 21, 24, 29]. Robustness issues are particularly critical for light and/or small vehicles, like blimps and reduced-scale VTOL vehicles, very sensitive to wind-induced

perturbations. The last decades have witnessed an increasing interest in the construction of these vehicles and the development of specific control approaches for autonomous navigation. Let us mention the examples of the HoverEye [5, 6, 23, 24], X4-flyer [11, 30], iStar [16], or AVATAR [27] VTOL vehicles, and the AURORA airship [2, 20]. This interest is much related to the versatility of these systems for surveillance and inspection missions, and to the development of low-cost and low-weight embarked sensors (Inertial Measurement Units, cameras, etc.). However, nonlinear control studies focusing on robustness issues for these systems, like [2, 20, 24] for instance, are not numerous. The present paper is also a contribution to the design and analysis of robust nonlinear control laws.

The control design framework here proposed applies to a large class of underactuated vehicles and several control modes typically associated with different levels of motion autonomy. Particular attention is paid to the three following problems: i) stabilization of (desired) reference thrust directions, ii) stabilization of reference linear velocities, and iii) stabilization of reference position-trajectories. The first and second problems relate typically to manual joystick-augmented-control situations, whereas the third one is associated with fully autonomous motion applications. In this paper, we consider the case of vehicles moving in 3D-space with four independent actuators (one force and three torques), knowing that six actuators would be necessary for full actuation. At the first glance, the proposed approach is reminiscent of methods described in [9, 24, 28] for the stabilization of hovering VTOL vehicles, based on the idea of using the thrust force and the vehicle's orientation as control variables to stabilize the vehicle's velocity and/or position; and then of applying a classical backstepping procedure or a high-gain controller to determine torque-inputs capable of stabilizing the desired orientation. In this paper, instead of the orientation, we use the vehicle's angular velocity as intermediary control input. This seemingly "small" difference is, in fact, consequential because it alleviates a certain number of difficulties associated with control inputs which belong to a compact manifold and enter the system's equation in a non-affine (nonlinear) manner. It also allows one to cast linear velocity and position control problems as natural extensions of the basic thrust direction control one. Another originality of this paper lies in the treatment of unmodeled dynamics. It is well-known from Control Theory that integral correction constitutes an effective means to compensate for modeling, measurement, and/or estimation static errors (biases). However, it is also well-known that this type of correction may generate so-called windup problems. Many control design techniques addressing these problems have been proposed during the last decades, like the nested saturations approach (see e.g. [10, 31]). These methods yield to bound integral correction terms in the control inputs. In doing so, the risk of saturating the actuators and jeopardizing the stability of the controlled system is reduced effectively. However, this does not prevent the integral terms themselves to grow arbitrarily large, nor the associated problem –little addressed in the literature– of slow desaturation which may increase the system's time response excessively. The nonlinear integrator bounding technique here proposed deals with this problem and is another contribution of the paper. Finally, the way energy dissipation produced by motion reaction forces is exploited, for both the control design and stability

analyses, constitutes to our knowledge a novel interpretation which justifies the use of simple models and supports observations made by other authors in this respect [26].

The paper is organized as follows. The notation and the dynamic modeling of the class of systems considered are recalled in Section 2. Some assumptions on the external forces applying to the system (gravity, aero/hydro-dynamic forces, etc.) are introduced and discussed in this section. Initial control laws are derived in Section 3 under assumptions upon the contribution of the external forces acting on the vehicle. The resulting simplification facilitates the exposition of the main lines of the approach. In Section 4, the controllers are modified in order to comply with more realistic assumptions. Simulation results for a particular model of a VTOL vehicle are described in Section 5 to illustrate the concepts. Finally, some remarks on the proposed control strategy and a discussion about possible future work conclude the paper.

Let us mention that a preliminary version [13] of this paper has been presented at the 46th IEEE–CDC. The present paper contains substantial extensions of the conference paper. In particular, *i*) the general case of vehicles moving in 3D-space is here considered, whereas [13] was limited to the planar case, *ii*) a control solution taking the constraint of unidirectional thrust into account is proposed (Section 3.5), *iii*) some control modifications are introduced to improve robustness properties w.r.t. some measurement or estimation errors (Section 4), *iv*) stability proofs for the proposed controllers are provided, and *v*) a case study is presented along with simulation results which illustrate the robustness of the approach w.r.t. unmodeled dynamics and perturbations (Section 5).

## 2 Notation and modeling

### 2.1 Notation

In this paper, we focus on vehicles which can be modeled as rigid bodies immersed in a fluid. The following notation is used.

- $G$  is the vehicle’s center of mass,  $m$  its mass, and  $J$  its inertia matrix.
- $\mathcal{I}=\{O; \vec{i}_o, \vec{j}_o, \vec{k}_o\}$  is a fixed (inertial or Galilean) frame w.r.t. (with respect to) which the vehicle’s absolute situation (position + orientation) is measured. This frame is chosen as the NED frame (North-East-Down) with the vector  $\vec{i}_o$  pointing to the North, the vector  $\vec{j}_o$  pointing to the East, and the vector  $\vec{k}_o$  pointing to the center of the earth.  $\mathcal{B}=\{G; \vec{i}, \vec{j}, \vec{k}\}$  is a frame attached to the body. The vector  $\vec{k}$  is parallel to the thrust force axis. This leaves two possible and opposite directions for this vector. In practice, selecting one of them can be related to considering a “nominal” motion associated with the vehicle and choosing the direction which makes the scalar product between the thrust force vector and  $\vec{k}$  either positive or negative. Whereas the positive option would correspond to the heading direction of a ship moving forward, we have opted here for the negative one in order to be consistent with the convention used for VTOL vehicles (with  $\vec{k}$  pointing downward nominally).



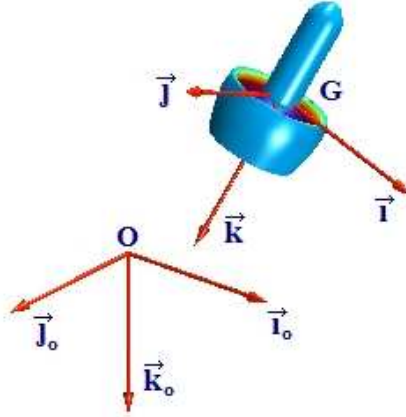


Figure 1: Inertial and body-fixed frames.

- The vector of coordinates of  $G$  in the basis of the fixed frame  $\mathcal{I}$  is denoted as  $x = (x_1, x_2, x_3)^T$  with the  $\mathbf{T}$ -symbol used for the operation of transposition. Therefore,  $\overrightarrow{OG} = x_1 \overrightarrow{i}_o + x_2 \overrightarrow{j}_o + x_3 \overrightarrow{k}_o$ , a relation that we will also write in a more concise way as  $\overrightarrow{OG} = (\overrightarrow{i}_o, \overrightarrow{j}_o, \overrightarrow{k}_o)x$ .
- The orientation of the body-fixed frame  $\mathcal{B}$  w.r.t. the inertial frame  $\mathcal{I}$  is represented by the rotation matrix  $R$ . The column vectors of  $R$  correspond to the vectors of coordinates of  $\overrightarrow{i}$ ,  $\overrightarrow{j}$ ,  $\overrightarrow{k}$  expressed in the basis of  $\mathcal{I}$ .
- The vector of coordinates associated with the linear velocity of  $G$  w.r.t.  $\mathcal{I}$  is denoted as  $\dot{x} = (\dot{x}_1, \dot{x}_2, \dot{x}_3)^T$  when expressed in the basis of  $\mathcal{I}$ , and as  $v = (v_1, v_2, v_3)^T$  when expressed in the basis of  $\mathcal{B}$ , i.e.  $\overrightarrow{v} = \frac{d}{dt}\overrightarrow{OG} = (\overrightarrow{i}_o, \overrightarrow{j}_o, \overrightarrow{k}_o)\dot{x} = (\overrightarrow{i}, \overrightarrow{j}, \overrightarrow{k})v$ .
- The angular velocity vector of the body-fixed frame  $\mathcal{B}$  relative to the fixed frame  $\mathcal{I}$ , expressed in  $\mathcal{B}$ , is denoted as  $\omega = (\omega_1, \omega_2, \omega_3)^T$ .
- The ambient fluid velocity w.r.t. the fixed frame  $\mathcal{I}$  is denoted as  $\overrightarrow{v}_f = (\overrightarrow{i}_o, \overrightarrow{j}_o, \overrightarrow{k}_o)\dot{x}_f = (\overrightarrow{i}, \overrightarrow{j}, \overrightarrow{k})v_f$ .
- The “apparent velocity” of the body  $\overrightarrow{v}_a$  is the difference between the velocity of  $G$  and the ambient fluid velocity, i.e.  $\overrightarrow{v}_a = \overrightarrow{v} - \overrightarrow{v}_f$ . Its vector of coordinates is  $\dot{x}_a = \dot{x} - \dot{x}_f$  expressed in the basis of the fixed frame  $\mathcal{I}$ , and  $v_a = v - v_f$  expressed in the basis of the body-fixed frame  $\mathcal{B}$ , i.e.  $\overrightarrow{v}_a = (\overrightarrow{i}_o, \overrightarrow{j}_o, \overrightarrow{k}_o)\dot{x}_a = (\overrightarrow{i}, \overrightarrow{j}, \overrightarrow{k})v_a$ .

- $\{e_1, e_2, e_3\}$  denotes the canonical basis of  $\mathbb{R}^3$ , i.e.  $e_1 = (1, 0, 0)^T$ ,  $e_2 = (0, 1, 0)^T$ ,  $e_3 = (0, 0, 1)^T$ .
- For any vector  $u \in \mathbb{R}^3$ ,  $S(u)$  denotes the skew-symmetric matrix associated with the cross product by  $u$ , i.e.  $S(u)v = u \times v$  for any vector  $v \in \mathbb{R}^3$ , with  $\times$  the cross-product operation.
- The Euclidean norm in  $\mathbb{R}^3$  is denoted as  $|\cdot|$ .
- A function  $y : [t_o, +\infty) \rightarrow \mathbb{R}^p$  is u.b. (for *ultimately bounded*) by a constant  $c$ , if there exists a time  $T$  such that  $|y(t)| \leq c$ ,  $\forall t \geq T$ . An output  $y = h(x, t) \in \mathbb{R}^p$  is u.u.b. (for *uniformly ultimately bounded*) by a constant  $c$  along the solutions to a differential equation  $\dot{x} = f(x, t)$  if, for any  $(x_o, t_o)$ ,  $y(\cdot) = h(x(\cdot, x_o, t_o))$  is u.b. by  $c$ , where  $x(\tau, x_o, t_o)$  denotes the solution at time  $\tau$  of  $\dot{x} = f(x, t)$  with initial condition  $x_o$  at  $t = t_o$ .

## 2.2 System modeling

We consider mechanical systems with four control inputs: one force input  $T$  (also referred to as the “thrust” input) along the body-fixed direction  $\vec{k}$  to create longitudinal motion, and three independent torque inputs to create rotational motion and monitor the vehicle’s attitude. This corresponds to a typical arrangement that can be found on VTOL vehicles, airplanes, blimps, rockets, etc. We assume that the thrust  $\vec{T} = -T\vec{k}$  applies at a point little distant from the axis  $\{G; \vec{k}\}$  so that it does not create an important torque at  $G$ . The torque actuation is typically obtained via secondary propellers (X4-Flyer), rudders or flaps (HoverEye), control moment gyros (see [32]), etc. Complete torque actuation allows to modify the vehicle’s attitude in order to direct the thrust at will. All the other forces acting on the vehicle (gravity and buoyancy forces, added-mass forces, and dissipative aerodynamic or hydrodynamic reaction forces) are summed up in a vector  $\vec{F}_e$ , so that the total resultant force applied to the vehicle is

$$\vec{F} = -T\vec{k} + \vec{F}_e$$

In the absence of motion reaction forces exerted by the ambient fluid on the vehicle, only gravity, eventually counteracted by buoyancy forces of roughly constant magnitude, are present in  $\vec{F}_e$ . This force can then be modeled as a constant vector parallel to the  $\{0; \vec{k}_o\}$  axis associated with the fixed frame  $\mathcal{I}$ . However, due to aerodynamic or hydrodynamic reaction forces, this vector generally depends on the apparent body velocity and acceleration (via added-mass effects), i.e. on  $(\dot{x}_a, \ddot{x}_a, \omega, \dot{\omega})$  as well as on the vehicle’s attitude  $R$ . It may also depend on the vehicle’s position when the characteristics of the ambient fluid are not the same everywhere. For simplicity, this latter dependence will not be considered in this paper. Moreover, whereas the dependence on accelerations is roughly linear, it is known that the intensities of motion reaction forces vary like the square of  $|\dot{x}_a|$ . Therefore, the intensity and direction of  $\vec{F}_e$  can vary in large proportions as soon as the vehicle’s desired velocity is

modified significantly, or due to important modifications of the ambient environment (waves, wind gusts, etc.). Modeling the various components of this function is, in general, time consuming and costly. This modeling effort is necessary for simulation purposes, and also for the optimization of the vehicles' geometrical and mechanical characteristics. A model of  $\vec{F}_e$  can also be of use for control design purposes. However, the knowledge of a precise and well-tuned model may not be as critically important as for simulation. Two classical reasons are that i) a well-designed feedback control is expected to grant robustness -in the sense of performance insensitivity- w.r.t. model inaccuracies, and ii) using on-line measurements or, more realistically, estimations of  $\vec{F}_e$  based on a crude model, in the control can be preferable to using a sophisticated but nonetheless imperfect functional model of this force. In [13], an estimation of  $\vec{F}_e$  based on the measurement of the vehicle's velocities and a high gain observer is proposed. Since there exists a variety of solutions to this problem, we henceforth assume that  $\vec{F}_e$  and its time-derivative are measured and/or estimated with good accuracy. Although the present paper focuses on control aspects almost exclusively, we are aware that, for many applications, estimation issues in relation to the design and use of adequate sensors are complementary and critically important.

Applying the fundamental theorem of Mechanics (Newton's second law) in the coordinates  $x$  yields

$$m\ddot{x} = -TRe_3 + F_e(\dot{x}, \ddot{x}, R, \omega, \dot{\omega}, t) \quad (1)$$

with  $F_e$  the components of  $\vec{F}_e$  in the inertial frame. By expressing the dynamics in the body-fixed frame  $\mathcal{B}$ , and by using Euler's theorem of angular momentum, one obtains the following equations

$$(\Sigma) : \begin{cases} (\Sigma_1) : \begin{pmatrix} \dot{x} \\ m\dot{v} \\ \dot{R} \end{pmatrix} = \begin{pmatrix} Rv \\ -mS(\omega)v - Te_3 + R^T F_e(\dot{x}, \ddot{x}, R, \omega, \dot{\omega}, t) \\ RS(\omega) \end{pmatrix} \\ (\Sigma_2) : J\dot{\omega} = -S(\omega)J\omega + \Gamma + \Gamma_e(\dot{x}, \ddot{x}, R, \omega, \dot{\omega}, t) \end{cases} \quad (2)$$

where  $\Gamma = (\Gamma_1, \Gamma_2, \Gamma_3)^T$  is the vector of torque inputs and  $\Gamma_e$  represents the external torque induced by the external forces.  $\Gamma_e$  is a "parasitic" torque in the sense that it is not easily controlled. For this reason, its components should at all times be kept smaller than the maximal amplitudes of the corresponding components of the control torque  $\Gamma$ . Accordingly, most vehicles are shaped so that the resultant torque of external forces acting on the vehicle is small (at least around nominal conditions of operation). Note however that this torque can also be used to provide the vehicle with desired properties in the absence of control action (when  $\Gamma = 0$ ). For instance, the weather helm tuning of a sailboat is directly related to this issue. And so is also the propensity of a plane to align its longitudinal axis with the apparent wind direction (stable state longitudinal mode), or to reduce the roll angle and maintain a horizontal straight flight (a safety feature for a number of cruise planes).

A rapid inspection of the system (2) shows that the dynamical subsystem  $(\Sigma_2)$  is fully-actuated. Exponential convergence of the angular velocity  $\omega$  to any bounded desired reference value is then theoretically possible especially when the external forces apply at points

close to the center of mass  $G$  and  $|\Gamma_e|$  is small and can be neglected. In this case, one may view  $\omega$  as an intermediary control input. In practice, this corresponds to the classical decoupled control architecture between inner and outer loops. The inner control loop provides high gain stabilization of the vehicle's angular velocity based on direct measurement of the angular velocity from the Inertial Measurement Unit. The outer control loop uses pose measurement along with estimation or measurement of the linear velocity as sensor inputs, and the angular velocity set point and thrust intensity as control inputs. For most applications, the time-scale separation between the two loops is sufficient to ensure that the interaction terms can be ignored in the control design. Therefore, in the sequel we consider  $T$  and  $\omega$  as the control inputs, and we focus on the control of the subsystem  $(\Sigma_1)$ .

### 2.3 Assumptions

To simplify both the control design and the associated analyses, we make some assumptions discussed hereafter.

**Assumption 1**  $F_e$  depends only on the vehicle's linear velocity  $\dot{x}$  and the independent time variable  $t$ . Moreover, it is continuously differentiable w.r.t. these variables, and the functions  $t \mapsto F_e(\dot{x}, t)$ ,  $t \mapsto \frac{\partial F_e}{\partial \dot{x}}(\dot{x}, t)$ , and  $t \mapsto \frac{\partial F_e}{\partial t}(\dot{x}, t)$  are bounded uniformly w.r.t.  $\dot{x}$  in compact sets.

The non-dependence of  $\vec{F}_e$  on the vehicle's attitude is physically justified when the aerodynamic (and/or hydrodynamic) forces do not depend on the vehicle's orientation, a property which depends essentially on the vehicle's shape. This assumption is clearly violated in the case of airplanes which are subjected to lift forces whose intensities are very sensitive to pitch angles, but it better holds in the case of VTOL vehicles, as exemplified by the "HoverEye" of Bertin Technologies Group. As for the non-dependence upon the angular velocity  $\omega$ , the assumption is better justified when i) the external forces apply at points close to the vehicle's center of mass, ii) motion reaction forces resulting from the vehicle's rotation can be neglected when compared to those produced by translational motion. Finally, the non-dependence on the acceleration variables  $\ddot{x}$  and  $\dot{\omega}$  is justified when added-mass effects can be neglected. These effects, which depend essentially on the ambient fluid characteristics, can be ignored when the density of the body is much more important than that of the environment. The example of a dense spherical body whose center coincides with its center of mass can be used to concretize a physical situation for which Assumption 1 holds with a good approximation.

The following two complementary assumptions are much less restrictive than the previous one. However, they are very important for the control design and analyses presented in Section 4.

**Assumption 2** There exist two real numbers  $c_1 \geq 0, c_2 > 0$  such that

$$|F_e(\dot{x}, t)| \leq c_1 + c_2 |\dot{x}|^2, \quad \forall (\dot{x}, t) \in \mathbb{R}^2 \times \mathbb{R} \quad (3)$$

**Assumption 3** *There exist two real numbers  $c_3 \geq 0, c_4 > 0$  such that*

$$\dot{x}^T F_e(\dot{x}, t) \leq c_3 |\dot{x}| - c_4 |\dot{x}|^3, \quad \forall (\dot{x}, t) \in \mathbb{R}^2 \times \mathbb{R} \quad (4)$$

Assumption 2 indicates that the intensity of  $\vec{F}_e$  cannot grow faster than the square of the intensity of the vehicle’s velocity vector. This is consistent with all common models of aerodynamic and hydrodynamic drag (and lift) forces. The constant  $c_1$  allows one to take the force of gravity into account, when it is active, as well as the action of perturbation forces produced by wind or sea-current. As for Assumption 3, it essentially accounts for the “dissipativity”, or “passivity”, property associated with drag forces. In particular, it says that for large velocities, the negative work of drag forces increases like the cube of the body’s apparent velocity and becomes predominant.

Finally, to avoid non-essential complications in the analyses, a last assumption is made; it is clearly little restrictive from an application viewpoint.

**Assumption 4** *The reference velocity  $\vec{v}_r$  is bounded in norm by a constant  $\bar{v}_r$ , and its first and second order time-derivatives  $\frac{d}{dt} \vec{v}_r$  and  $\frac{d^2}{dt^2} \vec{v}_r$  are well-defined and bounded.*

### 3 Basics of the control design

Using Assumption 1, the subsystem  $(\Sigma_1)$  of System (2) can be rewritten as

$$\begin{cases} \dot{x} &= Rv \\ \dot{v} &= -S(\omega)v - ue_3 + R^T \gamma_e(\dot{x}, t) \\ \dot{R} &= RS(\omega) \end{cases} \quad (5)$$

with  $\gamma_e(\dot{x}, t) := F_e(\dot{x}, t)/m$  called the “apparent acceleration”, and  $u := T/m$  and  $\omega$  used hereafter as the control inputs.

This section is devoted to the stabilization of either the vehicle’s thrust direction, or its linear velocity, or its position. The angular velocity  $\omega_3$  about the thrust axis is not involved in the realization of these control objectives, so that this degree of freedom can be used for complementary objectives and defined case-by-case depending on the considered vehicle and application. *A priori*, there are infinitely many possibilities at this level, starting with the simplest choice  $\omega_3 = 0$ . In [22] (pages 105–108) this variable is determined in order to take advantage of lift forces associated with an asymmetric VTOL vehicle. In the sequel, to simplify the control design and the associated analyses, we just assume that  $\omega_3(t)$  is well-defined at any time and bounded.

#### 3.1 Thrust direction control

Let  $\gamma \in \mathbb{R}^3$  denote a unit vector ( $|\gamma| = 1$ ) associated with the desired (possibly varying) thrust direction and expressed in the inertial frame  $\mathcal{I}$ . In practice, this desired direction may correspond to the one specified by a manual joystick. The objective is the stabilization of

the vehicle's thrust direction about the reference vector  $\gamma$  or, equivalently, the stabilization of  $R^T\gamma$  about  $e_3$ .

Define

$$\bar{\gamma} := R^T\gamma \quad (6)$$

and let  $\tilde{\theta} \in (-\pi; \pi]$  denote the angle between the two unit vectors  $e_3$  and  $\bar{\gamma}$ , so that  $\cos \tilde{\theta} = \bar{\gamma}_3$ , the third component of  $\bar{\gamma}$ . The control objective is also equivalent to the asymptotic stabilization of  $\tilde{\theta} = 0$ . Based on the above notation, the first control result of this paper is stated next.

**Proposition 1** *Let  $k$  denote a strictly positive constant, and apply the control law*

$$\begin{cases} \omega_1 &= -\frac{k\bar{\gamma}_2}{(1+\bar{\gamma}_3)^2} - \gamma^T S(Re_1)\dot{\gamma} \\ \omega_2 &= \frac{k\bar{\gamma}_1}{(1+\bar{\gamma}_3)^2} - \gamma^T S(Re_2)\dot{\gamma} \end{cases} \quad (7)$$

to the system  $\dot{R} = RS(\omega)$ . Then the equilibrium point  $\tilde{\theta} = 0$  of the resulting closed-loop system is exponentially stable with domain of attraction equal to  $(-\pi, \pi)$ .

The proof of this proposition is given in Appendix A.1. In what follows, we show how this controller can be extended to the linear velocity and position control problems.

### 3.2 Velocity control

Let  $\dot{x}_r$  denote the reference velocity expressed in the inertial frame  $\mathcal{I}$ ,  $\ddot{x}_r$  the time-derivative of  $\dot{x}_r$ , and  $\tilde{v} := R^T(\dot{x} - \dot{x}_r)$  the velocity error term expressed in the body-fixed frame  $\mathcal{B}$ . Instead of defining  $\gamma$  as a reference unit vector as in the previous subsection, we now define

$$\gamma(\dot{x}, t) := \gamma_e(\dot{x}, t) - \ddot{x}_r(t) \quad (8)$$

One then obtains the following error model

$$\dot{\tilde{x}} = R\tilde{v} \quad (9a)$$

$$\dot{\tilde{v}} = -S(\omega)\tilde{v} - ue_3 + R^T\gamma(\dot{x}, t) \quad (9b)$$

$$\dot{R} = RS(\omega) \quad (9c)$$

with either  $\tilde{x} := \int_0^t (\dot{x}(s) - \dot{x}_r(s)) ds$ , the integral of the velocity error, or  $\tilde{x} := x - x_r$ , the position tracking error when a reference trajectory  $x_r$  is specified.

The problem of asymptotic stabilization of the linear velocity error  $\dot{x} - \dot{x}_r$  to zero is clearly equivalent to the asymptotic stabilization of  $\tilde{v}$  to zero. Equation (9b) indicates that  $\tilde{v} \equiv 0$  implies that

$$-ue_3 + R^T\gamma(\dot{x}, t) = 0 \quad (10)$$

As long as  $\gamma(\dot{x}, t)$  is different from zero, it is possible to define a locally unique thrust direction solution to the above equation. However, this solution can not be prolonged by continuity at  $\gamma = 0$ . As a matter of fact, one can verify that this singularity corresponds to the case when the linearization of System (9b)–(9c) at any equilibrium point  $(\tilde{v}, R) = (0, R^*)$  is not controllable. Very specific (and still prospective) nonlinear control techniques are required to address stabilization issues in this case (see e.g. [19]). These techniques are not the subject of the present paper because the vanishing of  $\gamma$  does not correspond to a generic situation for a large class of underactuated mechanical systems (those for which  $\gamma_e(\dot{x}_r(t), t)$  is nominally different from zero). We essentially discard this difficult case here by assuming that

**Assumption 5** *There exists  $\delta > 0$  such that, for all  $(\dot{x}, t)$ ,  $|\gamma(\dot{x}, t)| \geq \delta$ .*

Although this assumption is restrictive, it simplifies the exposition of a basic and generic control design. In Section 4, however, we will weaken this assumption and propose an ad-hoc adaptation of the control design in order to ensure the well-posedness of the controller's expression and maintain a minimal control of the vehicle when  $|\gamma|$  gets close to zero. When both Assumption 5 and relation (10) hold, using (6) one deduces that

$$\bar{\gamma} = \pm |\gamma| e_3.$$

Let  $\tilde{\theta} \in (-\pi; \pi]$  denote the angle between the two unit vectors  $e_3$  and  $\frac{\bar{\gamma}}{|\bar{\gamma}|}$ , so that  $\cos \tilde{\theta} = \frac{\bar{\gamma}_3}{|\bar{\gamma}|}$ . The control objective implies that either  $\tilde{\theta} = 0$  (i.e.  $\bar{\gamma} = |\gamma| e_3$ ) or  $\tilde{\theta} = \pi$  (i.e.  $\bar{\gamma} = -|\gamma| e_3$ ) must be asymptotically stabilized. The choice between these two equilibria is often made via simple physical considerations such as minimizing the energy consumption in relation to actuator's efficiency and vehicle's shape, or by taking into account the unilaterality of the thrust direction as in the case of most VTOL vehicles. Without loss of generality, we henceforth assume that the choice has been made to stabilize  $\tilde{\theta} = 0$ .

Based on the above notation, the second control result of this paper is stated in the next proposition.

**Proposition 2** *Let  $k_1, k_2, k_3$  denote strictly positive constants, and apply the control law*

$$\begin{cases} u &= \bar{\gamma}_3 + |\gamma| k_1 \tilde{v}_3 \\ \omega_1 &= -|\gamma| k_2 \tilde{v}_2 - \frac{k_3 |\gamma| \tilde{\gamma}_2}{(|\gamma| + \bar{\gamma}_3)^2} - \frac{1}{|\gamma|^2} \gamma^T S(R e_1) \dot{\gamma} \\ \omega_2 &= |\gamma| k_2 \tilde{v}_1 + \frac{k_3 |\gamma| \tilde{\gamma}_1}{(|\gamma| + \bar{\gamma}_3)^2} - \frac{1}{|\gamma|^2} \gamma^T S(R e_2) \dot{\gamma} \end{cases} \quad (11)$$

to System (9). Suppose that Assumptions 1, 4, and 5 are satisfied. Then, for the subsystem (9b)–(9c), the equilibrium point  $(\tilde{v}, \tilde{\theta}) = (0, 0)$  of the closed-loop system is asymptotically stable with domain of attraction equal to  $\mathbb{R}^3 \times (-\pi, \pi)$ .

The proof of this proposition is given in Appendix A.2. It is based on the use of the candidate Lyapunov function

$$V = \frac{1}{2} \tilde{v}^T \tilde{v} + \frac{1}{k_2} \left( 1 - \frac{\tilde{\gamma}_3}{|\tilde{\gamma}|} \right) = \frac{1}{2} \tilde{v}^T \tilde{v} + \frac{1}{k_2} (1 - \cos \tilde{\theta}) \quad (12)$$

whose time-derivative is shown to be negative semi-definite along any solution of the closed-loop system.

### 3.3 Velocity control with integral term

For the stability and convergence analysis of the control (11), it is implicitly assumed that  $\gamma(\dot{x}, t) = \gamma_e(\dot{x}, t) - \ddot{x}_r(t)$  is perfectly known. In practice however, due in particular to the difficulty of obtaining precise measures or estimates of  $F_e$ , the apparent acceleration  $\gamma_e$  is not known exactly. Nor is  $\gamma$  therefore. It is well-known from the control theory of linear systems that the incorporation of integral correction terms in the control design can compensate for additive perturbations which, in the present case, may take the form of a constant bias in the measurement (or estimation) of  $\gamma_e$ . The objective of this subsection is to show that the control (11) can be modified in order to still ensure the convergence of  $\dot{x} - \dot{x}_r$  to zero when such a bias is present. To this purpose, let us introduce the following integral term

$$I_v(t) := \int_0^t (\dot{x}(s) - \dot{x}_r(s)) ds + I_0 \quad (13)$$

where  $I_0$  is an arbitrary constant. Also, let  $h$  denote a smooth bounded strictly positive function defined on  $[0, +\infty)$  such that, for some positive constants  $\eta, \beta$ ,

$$\forall s > 0, \quad h(s^2)s < \eta \quad (14)$$

$$\forall s \in \mathbb{R}, \quad 0 < \frac{\partial}{\partial s}(h(s^2)s) < \beta \quad (15)$$

An example of such a function is  $h : s \mapsto h(s) = \frac{\eta}{\sqrt{1+s}}$ , with  $\eta$  a positive constant. Let  $\hat{\gamma}_e$  denote the measure (or estimate) of  $\gamma_e$  and define now  $\gamma$  as follows (in replacement of relation (8))

$$\gamma := \hat{\gamma}_e - \ddot{x}_r + h(|I_v|^2)I_v \quad (16)$$

**Proposition 3** *Apply the control law (11) to System (9) with  $\gamma$  defined by (16). Suppose that*

- i) Assumptions 1, 4, and 5 are satisfied,*
- ii) the measurement (or estimation) error  $c := \gamma_e - \hat{\gamma}_e$  is constant,*



$$iii) \lim_{s \rightarrow +\infty} h(s^2)s > |c|.$$

Then, for System (9b)–(9c) complemented with the equation  $\dot{I}_v = R\tilde{v}$ , there exists a constant vector  $I_v^* \in \mathbb{R}^3$  such that the equilibrium point  $(I_v, \tilde{v}, \tilde{\theta}) = (I_v^*, 0, 0)$  of the closed-loop system is asymptotically stable, with domain of attraction equal to  $\mathbb{R}^3 \times \mathbb{R}^3 \times (-\pi, \pi)$ .

The proof of this proposition is similar to the proof of Proposition 2. Complementary details are given in Appendix A.3.

Let us briefly comment on the role of the function  $h$  and its properties. The property (14) of  $h$  is introduced in order to limit, via (16), the influence of the integral  $I_v$  in the control action. However, Assumption *iii)* of Proposition 3 also points out that the upper-bound  $\eta$  associated with the choice of this function should not be too small in order to compensate for a large estimation error  $c$ . On the other hand, in view of (16), a small value for  $\eta$  may reduce the risk of having  $|\gamma|$  getting close to zero. This policy leads, for instance, to choose  $\eta < g$  in the case when  $\gamma_e$  is essentially equal to the gravity acceleration, and the estimation error  $c$  and  $\ddot{x}_r$  are small compared to this acceleration. These considerations illustrate that a compromise has to be found, depending on the considered vehicle and application.

### 3.4 Position control

The third control objective is the combined stabilization of the velocity error  $\tilde{v}$  (or  $\dot{x} - \dot{x}_r$ ) and the position error  $\tilde{x} = x - x_r$  to zero. A first solution to this problem is provided by the control proposed in the previous subsection since, by setting  $I_0 = x(0) - x_r(0)$  in (13), one has  $I_v = \tilde{x}$ . Now, alike the velocity stabilization case, it can be useful (and even necessary) in practice to complement the control action with a position error integral correction term. A possibility consists in using a term proportional to the output  $z$  of a classical integrator of  $\tilde{x}$  (i.e.  $\dot{z} = \tilde{x}$ ) in the control expression. However, this solution presents several drawbacks. For example, the integral correction term may grow very large and this may in turn cause large overshoots of the position tracking error. To avoid this problem, and also cope with actuator limitations, one has to saturate the integral term. This can be done in many ways, some better than others. For instance, it matters to prevent the so-called desaturation (or windup) problem from occurring in order to not overly increase the system's time response. The solution proposed in this paper is based on a nonlinear dynamical extension yielding a type of bounded nonlinear integrator. More precisely, we denote  $z$  the solution to the following differential equation driven by  $\tilde{x}$

$$\ddot{z} = -2k_z \dot{z} - k_z^2(z - \text{sat}_\Delta z) + k_z h_z(|\tilde{x}|^2)\tilde{x} \quad (k_z > 0, \quad z(0) = 0) \quad (17)$$

where  $h_z$  denotes a smooth bounded strictly positive function satisfying (14)–(15) for some positive constants  $\eta_z, \beta_z$ , and  $\text{sat}_\Delta$  is a continuous “saturation function” characterized by the following properties, with  $\Delta$  a positive number associated with this function,

*P1.*  $\text{sat}_\Delta$  is right-differentiable along any smooth curve, and its derivative is bounded.

P2.  $\forall x \in \mathbb{R}^3$ , if  $|x| \leq \Delta$ ,  $\text{sat}_\Delta(x) = x$ .

P3.  $\exists \bar{\Delta} > 0$  such that  $\forall x \in \mathbb{R}^3$ ,  $|\text{sat}_\Delta(x)| \leq \bar{\Delta}$ .

P4.  $\forall (c, x) \in \mathbb{R}^3 \times \mathbb{R}^3$  such that  $|c| < \Delta$ ,  $|\text{sat}_\Delta(x + c) - c| \leq |x|$ .

A possible choice is the classical saturation function defined as

$$\text{sat}_\Delta(x) := x \min\left(1, \frac{\Delta}{|x|}\right) \quad (\Delta > 0) \quad (18)$$

for which  $\Delta = \bar{\Delta}$ .

One verifies from (17) that ultimate uniform upper-bounds of  $|z|$ ,  $|\dot{z}|$ , and  $|\ddot{z}|$  are  $\bar{\Delta} + \eta_z/k_z$ ,  $2(k_z\bar{\Delta} + \eta_z)$ , and  $6k_z(k_z\bar{\Delta} + \eta_z)$  respectively.

Define

$$y := \tilde{x} + z \quad (19)$$

$$\bar{v} := \tilde{v} + R^T \dot{z} \quad (20)$$

$$\gamma := \hat{\gamma}_e - \ddot{x}_r + h(|y|^2)y + \ddot{z} \quad (21)$$

where  $\hat{\gamma}_e$  denotes the measurement (or estimation) of  $\gamma_e$ , and  $h$  is a smooth bounded strictly positive function satisfying (14)–(15)<sup>1</sup> for some constants  $\eta, \beta > 0$ .

**Proposition 4** *Let  $k_1, k_2, k_3$  denote strictly positive constants. Apply the following control law*

$$\begin{cases} u &= \bar{\gamma}_3 + |\gamma|k_1\bar{v}_3 \\ \omega_1 &= -|\gamma|k_2\bar{v}_2 - \frac{k_3|\gamma|\bar{\gamma}_2}{(|\gamma| + \bar{\gamma}_3)^2} - \frac{1}{|\gamma|^2}\gamma^T S(Re_1)\dot{\gamma} \\ \omega_2 &= |\gamma|k_2\bar{v}_1 + \frac{k_3|\gamma|\bar{\gamma}_1}{(|\gamma| + \bar{\gamma}_3)^2} - \frac{1}{|\gamma|^2}\gamma^T S(Re_2)\dot{\gamma} \end{cases} \quad (22)$$

to System (9) with  $\bar{v}$ ,  $\gamma$ , and  $y$  (which intervenes in the definition of  $\gamma$ ) defined by (20), (21), and (19) respectively. Suppose that

- i) Assumptions 1, 4, and 5 are satisfied,
- ii) the measurement (or estimation) error  $c := \gamma_e - \hat{\gamma}_e$  is constant,
- iii)  $\lim_{s \rightarrow +\infty} h(s^2)s > |c|$ ,
- iv)  $\Delta > |z^*|$ , where  $z^*$  denote the unique solution to the equation  $h(|z^*|^2)z^* = c$ .

<sup>1</sup>Note that  $h$  can be different from  $h_z$ .

Then, for System (9) complemented with (17), the equilibrium point  $(z, \dot{z}, \tilde{x}, \tilde{v}, \tilde{\theta}) = (z^*, 0, 0, 0, 0)$  of the closed-loop system is asymptotically stable, with domain of attraction equal to  $\mathbb{R}^3 \times \mathbb{R}^3 \times \mathbb{R}^3 \times (-\pi, \pi)$ .

The proof of this proposition is given in Appendix A.4.

The role of the function  $h$  has been commented upon in the previous subsection. For position stabilization, we further remark that the property (14) of  $h$  bounds the contribution of the position error  $\tilde{x}$  in  $\gamma$  defined by (21), and thus also in the control inputs defined by (22). This limits the influence of large initial position errors on the control inputs intensity, and reduces the risk of saturating the actuators. Note that the choice of  $h$  is still a matter of compromise. Let us comment on the role of the coefficient  $k_z$ . Equation (17) points out that  $k_z$  influences the rate of desaturation of  $z$  which can be observed, for instance, when  $|z|$  is initially larger than  $\Delta$  and  $\tilde{x} = 0$ . The larger  $k_z$ , the faster the desaturation and the smaller the influence of this integral action on the system's time response. On the other hand, since upper-bounds of  $|\dot{z}|$  and  $|\gamma|$  are proportional to  $k_z$ , a "small" value of  $k_z$  tends to limit the risk of saturating the actuators. A large value of  $k_z$  also increases the range interval of  $|\gamma|$  and, subsequently, the risk of getting  $|\gamma|$  close to zero (a value for which the control is no longer defined). The tuning of  $k_z$  is thus again a matter of compromise to be solved case-by-case depending on the considered vehicle and application.

### 3.5 Control with unidirectional thrust

In many applications the thrust direction cannot be inverted. This means that only a positive (resp. negative) or null control  $u$  can be applied. For the control laws given in Propositions 2–4, this sign constraint is satisfied in the neighborhood of the stabilized equilibrium point (since  $u \approx |\gamma|$  and  $|\gamma| > 0$  from Assumption 5). However it is not satisfied in the entire domain of attraction of this equilibrium. The following proposition points out how the position control law (22) in Proposition 4 can be modified to comply with the constraint  $u \geq 0$ , without consequences on the stability issue.

**Proposition 5** *Let  $k_1, k_2, k_3$  denote strictly positive constants, and  $\bar{v}$  and  $\gamma$  as defined in Proposition 4. Let  $\sigma : \mathbb{R} \rightarrow \mathbb{R}$  denote a strictly increasing smooth function such that  $\sigma(0) = 0$  and  $\sigma(s) > -\frac{1}{k_1}, \forall s \in \mathbb{R}$ . Apply the control law*

$$\begin{cases} u &= |\gamma| + |\gamma|k_1\sigma(\bar{v}_3) \quad (\geq 0) \\ \omega_1 &= -|\gamma|k_2 \left( \bar{v}_2 - \bar{v}_3 \frac{\bar{\gamma}_2}{|\gamma| + \bar{\gamma}_3} \right) - \frac{k_3|\gamma|\bar{\gamma}_2}{(|\gamma| + \bar{\gamma}_3)^2} - \frac{1}{|\gamma|^2} \gamma^T S(Re_1) \dot{\gamma} \\ \omega_2 &= |\gamma|k_2 \left( \bar{v}_1 - \bar{v}_3 \frac{\bar{\gamma}_1}{|\gamma| + \bar{\gamma}_3} \right) + \frac{k_3|\gamma|\bar{\gamma}_1}{(|\gamma| + \bar{\gamma}_3)^2} - \frac{1}{|\gamma|^2} \gamma^T S(Re_2) \dot{\gamma} \end{cases} \quad (23)$$

to System (9). Suppose that Assumptions i)–v) of Proposition 4 are satisfied. Then the asymptotic stability result of Proposition 4 still holds.

The proof of this proposition is given in Appendix A.5. Note that the proposed modification of the control law applies as well to the control laws of Propositions 2 and 3 by simply replacing  $\bar{v}$  in the control expression (23) by  $\tilde{v}$ . Possible choices for the function  $\sigma$  are given, e.g., by

$$\sigma(s) = \frac{\alpha}{k_1} \tanh\left(\frac{k_1 s}{\alpha}\right), \text{ or } \sigma(s) = \frac{s}{\sqrt{1 + \frac{k_1^2 s^2}{\alpha^2}}}$$

with  $0 < \alpha \leq 1$ .

## 4 Control robustification

The results of the previous section rely upon the satisfaction of Assumption 5 which unconditionally guarantees the existence and local uniqueness of the desired thrust direction in the velocity and position control cases. For most underactuated vehicles, this assumption is not satisfied. Let us illustrate this on a simple example.

**Example 1** (Spherical vehicle) Consider a spherical vehicle, with its center of mass coinciding with the sphere's center, submitted to the action of gravity, drag forces, and added-mass effects. The translational dynamics of the vehicle is given by (1) with  $F_e(\dot{x}, \ddot{x}) = -c_a |\dot{x}| \dot{x} - m_a \ddot{x} + m g e_3$ , and  $c_a, m_a$  positive constant numbers associated with drag forces and added-mass effects respectively. This equation can be rewritten as (compare with (1))  $\bar{m} \ddot{x} = -T R e_3 + \bar{F}_e(\dot{x})$  with  $\bar{m} = m + m_a$ , and  $\bar{F}_e(\dot{x}) = -c_a |\dot{x}| \dot{x} + m g e_3$ . The term  $\gamma(\dot{x}, t)$  of equation (8) is thus given by

$$\gamma(\dot{x}, t) = \frac{\bar{F}_e(\dot{x})}{\bar{m}} - \ddot{x}_r = -\frac{c_a}{\bar{m}} |\dot{x}| \dot{x} + \frac{m g}{\bar{m}} e_3 - \ddot{x}_r$$

When drag effects can be neglected (i.e.  $\frac{c_a}{\bar{m}} |\dot{x}| \dot{x} \approx 0$ ), Assumption 5 is not satisfied when the reference acceleration vector  $\ddot{x}_r$  is equal to  $\frac{m g}{\bar{m}} e_3$ . As a matter of fact, the above relation points out that there always exists a velocity  $\dot{x}$  such that  $\gamma(\dot{x}, t) = 0$ .

Another example where Assumption 5 is not satisfied is provided by a ship drifting with the sea current at zero relative velocity. Indeed, the sum of external forces applied to the ship is equal to zero in this case. Even though one may hope that the set of "bad" velocities does not belong to the nominal operational domain of the vehicle, these examples indicate that, in some cases, Assumption 5 is too strong. Moreover, when it is violated, the control is no longer defined. Now, to ensure *local* stability, it is sufficient that  $\gamma$  does not vanish near the considered reference velocity  $\dot{x}_r$ . This suggests to replace Assumption 5 by the following weaker assumption.

**Assumption 6** *There exists  $\delta > 0$  such that, for all  $t$ ,  $|\gamma(\dot{x}_r(t), t)| \geq \delta$ .*

Under this assumption, the control laws proposed in Section 3 are locally well-defined and ensure *local* asymptotic stability of the desired reference velocity/position trajectory. This

may be sufficient for many applications. However, for practical purposes one would like to stay on the safe side and ensure that, for instance, the control calculation is always well-posed and that the tracking errors resulting from the control action can never diverge explosively, whatever the adverse environmental conditions or poorly chosen reference trajectories for which  $\gamma$  approaches the null vector at some time-instant. Accordingly, the objective of this section is to modify the controllers of Section 3 in order to have the three following properties satisfied simultaneously:

- P1)* local asymptotic stability when Assumption 6 is satisfied,
- P2)* well-posedness of the expressions of the control inputs even when Assumption 6 is not satisfied,
- P3)* global uniform ultimate boundedness of the system's velocities  $\dot{x}$  and  $\omega$  even when Assumption 6 is violated.

The modifications are carried out for the velocity control objective of Proposition 2, but they are also valid for other control laws proposed in Section 3 modulo a straightforward transposition.

Property *P2)* is simply obtained by multiplying the unbounded terms  $1/|\gamma|$  and  $1/(|\gamma| + \bar{\gamma}_3)$  in the control expression (11) by an adequate function taking the value one in the neighborhood of the reference trajectory and zero at  $\gamma = 0$ . For instance, one can use the  $C^1$  function  $\mu_\tau : [0, +\infty) \rightarrow [0, 1]$  defined by

$$\mu_\tau(s) = \begin{cases} \sin\left(\frac{\pi s^2}{2\tau^2}\right), & \text{if } s \leq \tau \\ 1, & \text{otherwise} \end{cases} \quad (24)$$

for some constant  $\tau > 0$ . This yields the modified control expression

$$\begin{cases} u &= \bar{\gamma}_3 + |\gamma|k_1\tilde{v}_3 \\ \omega_1 &= -|\gamma|k_2\tilde{v}_2 - \mu_\tau(|\gamma| + \bar{\gamma}_3)\frac{k_3|\gamma|\bar{\gamma}_2}{(|\gamma| + \bar{\gamma}_3)^2} - \mu_\tau(|\gamma|)\frac{1}{|\gamma|^2}\gamma^T S(Re_1)\dot{\gamma} \\ \omega_2 &= |\gamma|k_2\tilde{v}_1 + \mu_\tau(|\gamma| + \bar{\gamma}_3)\frac{k_3|\gamma|\bar{\gamma}_1}{(|\gamma| + \bar{\gamma}_3)^2} - \mu_\tau(|\gamma|)\frac{1}{|\gamma|^2}\gamma^T S(Re_2)\dot{\gamma} \end{cases} \quad (25)$$

This modification does not prevent Property *P1)* from being satisfied. On the other hand, the obtention of Property *P3)* is more involved. It relies in the first place on the following observation, which is a direct consequence of the dissipativity of drag forces (i.e. Assumption 3).

**Proposition 6** *Suppose that Assumption 3 is satisfied and that  $u$  is calculated according to a feedback law such that, for some constants  $\beta_1, \beta_2$ ,*

$$|u| \leq \beta_1 + \beta_2|\dot{x}| \quad (26)$$

*Then, the controlled vehicle's linear velocity  $\dot{x}$  is u.u.b.. Moreover, under Assumption 1,  $\gamma_e, \dot{\gamma}_e$  and the linear acceleration  $\ddot{x}$  are also u.u.b..*

**Proof** See Appendix A.6. ■

The objective is now to modify the expression (8) of  $\gamma(\dot{x}, t)$  so that  $u$ , as given by (25), can satisfy the property (26) without destroying the property of local asymptotic stability. To this purpose, let  $\overline{\text{sat}}_\Delta$  denote a continuous “saturation function” satisfying the Properties *P1*, *P2*, *P3* of the function  $\text{sat}_\Delta$  and also the following property

*P4*. There exists a continuous function  $\phi : \mathbb{R}^3 \rightarrow \mathbb{R}$  such that  $\forall (\xi, \gamma) \in \mathbb{R}^3 \times \mathbb{R}^3$ ,  $\phi(\gamma) \leq 1$  and

$$\xi^T \overline{\text{sat}}_\Delta(\gamma) = \phi(\gamma) \xi^T \gamma \quad (27)$$

A possible choice is the classical saturation function defined as

$$\overline{\text{sat}}_\Delta(\gamma) := \gamma \min \left( 1, \frac{\Delta}{|\gamma|} \right) \quad (28)$$

Let  $\gamma_d$  denote any 3-dimensional bounded  $\mathcal{C}^1$  time-dependent vector valued function whose derivative is also bounded. The role and choice of this function will be commented upon further, along with some examples. Define now  $\gamma$  as follows

$$\gamma(\dot{x}, t) := \gamma_d(t) + \overline{\text{sat}}_M(\gamma_{e,d}(\dot{x}, t)) - \ddot{x}_r(t) \quad (29)$$

with

$$\gamma_{e,d}(\dot{x}, t) := \gamma_e(\dot{x}, t) - \gamma_d(t) \quad (30)$$

From (29), Assumption 4, the boundedness of  $\gamma_d$ , and the boundedness of the function  $\overline{\text{sat}}_M$ , it follows that there exists a finite value  $Q > 0$  such that, whatever  $\dot{x}(t)$ ,

$$|\gamma(\dot{x}(t), t)| \leq Q \quad (31)$$

Therefore, in view of the expression of  $u$  in (25), inequality (26) is now satisfied. Prior to stating the main stabilization result of this section, we need to introduce some extra notation. Since  $\gamma_d$  is bounded by assumption, it follows from Assumptions 2 and 3 (recall that  $\gamma_e = F_e/m$ ) and (30) that there exist constant numbers  $\bar{c}_1 \geq 0$ ,  $\bar{c}_2 > 0$ ,  $\bar{c}_3 \geq 0$ ,  $\bar{c}_4 > 0$  such that,  $\forall (\dot{x}, t) \in \mathbb{R}^3 \times \mathbb{R}$ ,

$$\begin{cases} |\gamma_{e,d}(\dot{x}, t)| & \leq \bar{c}_1 + \bar{c}_2 |\dot{x}|^2 \\ \dot{x}^T \gamma_{e,d}(\dot{x}, t) & \leq \bar{c}_3 |\dot{x}| - \bar{c}_4 |\dot{x}|^3 \end{cases} \quad (32)$$

Consider the following polynomial in  $s$ , with  $\bar{\mathbf{v}}_r > 0$ ,

$$P(s) := \bar{c}_4 s^3 - \bar{c}_2 \bar{\mathbf{v}}_r s^2 - \bar{c}_3 s - \bar{c}_1 \bar{\mathbf{v}}_r$$

Since  $\bar{c}_4 > 0$ , there exists a number  $\kappa(\bar{c}_i, \bar{\mathbf{v}}_r) \geq \bar{\mathbf{v}}_r$  such that  $s \geq \kappa(\bar{c}_i, \bar{\mathbf{v}}_r) \Rightarrow P(s) \geq 0$ .

The following theorem, whose proof is detailed in Appendix A.7, presents the main result of this section.

**Theorem 1** *Let  $k_1, k_2, k_3$  denote strictly positive constants. Apply the control law (25), with  $\mu_\tau$  and  $\gamma$  given by (24) and (29) respectively, to System (9). Suppose that  $0 < \tau < \delta$ , where  $\tau$  and  $\delta$  are the constants involved in relation (24) and Assumption 6 respectively. Suppose that Assumptions 1, 2, 3, 4, and 6 are satisfied. Then the following properties hold:*

- 1) *the control inputs  $u$  and  $\omega$  are well-defined and bounded along any system's solution,*
- 2)  *$\dot{x}$  is u.u.b. along any system's solution,*
- 3) *for the subsystem (9b)–(9c), the equilibrium point  $(\tilde{v}, \tilde{\theta}) = (0, 0)$  of the closed-loop system is locally asymptotically stable if  $M > \bar{c}_1 + \bar{c}_2 \bar{\mathbf{v}}_{\mathbf{r}}$ , with  $M$  the constant associated with the function  $\overline{\text{sat}}_M$  intervening in  $\gamma$ . Furthermore, if  $M \geq \bar{c}_1 + \bar{c}_2 (\kappa(\bar{c}_i, \bar{\mathbf{v}}_{\mathbf{r}}))^2$  and  $|\gamma(\dot{x}, t)| \geq \tau \forall (\dot{x}, t)$ , the attraction domain is equal to  $\mathbb{R}^3 \times (-\pi, \pi)$ .*

By comparison with the control laws of Section 3, the control (25) depends on extra design terms ( $\tau$ , and the functions  $\overline{\text{sat}}_M$  and  $\gamma_d$ ) which can be tuned so as to maximize the domain of stability of the closed-loop system. Let us illustrate this tuning possibility in the case of the spherical vehicle already considered in Example 1.

**Example 2** (Spherical vehicle, continued) To simplify, we assume that the desired velocity  $\dot{x}_r$  is constant, i.e.  $\ddot{x}_r = 0$ . In this case,  $\gamma_e(\dot{x}) = \gamma(\dot{x}) = \gamma_g + \gamma_{ae}(\dot{x})$ , with  $\gamma_g = (mg/\bar{m})e_3$  the gravity acceleration vector field, and  $\gamma_{ae}(\dot{x}) = -(c_a/\bar{m})|\dot{x}|\dot{x}$  ( $c_a > 0$ ) the acceleration vector associated with aerodynamic forces. Let us assume that the function  $\overline{\text{sat}}_M$  is defined by (28), and consider two possible choices for  $\gamma_d$  (among others). First, let  $\gamma_d = \gamma_g$ . Then  $\gamma = \gamma_g + \overline{\text{sat}}_M(\gamma_{e,d})$  and  $\gamma_{e,d} = \gamma_{ae}$ . Since the norm of  $\gamma_g$  is non-zero and constant, and  $\overline{\text{sat}}_M$  is bounded by  $M$ , Assumption 6 is satisfied if  $M < mg/\bar{m}$ . In this case  $|\gamma(\dot{x}, t)| \geq mg/\bar{m} - M > 0$ . Moreover, if  $\tau < mg/\bar{m} - M$ , the equilibrium  $(\tilde{v}, \tilde{\theta}) = (0, 0)$  is “globally” asymptotically stable (i.e. the domain of attraction is  $\mathbb{R}^3 \times (-\pi, \pi)$ ). However, imposing this inequality on  $M$  may not be compatible with the satisfaction of the condition  $M \geq \bar{c}_1 + \bar{c}_2 (\kappa(\bar{c}_i, \bar{\mathbf{v}}_{\mathbf{r}}))^2$  which guarantees the largest possible domain of attraction. Indeed, in this case one has  $\bar{c}_1 = \bar{c}_3 = 0$ ,  $\bar{c}_2 = \bar{c}_4 = c_a$ , and  $\kappa(\bar{c}_i, \bar{\mathbf{v}}_{\mathbf{r}}) = \bar{\mathbf{v}}_{\mathbf{r}}$ , so that the condition  $M \geq \bar{c}_1 + \bar{c}_2 (\kappa(\bar{c}_i, \bar{\mathbf{v}}_{\mathbf{r}}))^2$  is now equivalent to  $M \geq c_a \bar{\mathbf{v}}_{\mathbf{r}}^2$ . Therefore, the satisfaction of Assumption 6 and *global* asymptotic stability are guaranteed provided that

$$\sup |\dot{x}_r(t)| < \sqrt{mg/(\bar{m}c_a)} \quad (33)$$

Now, to stabilize larger reference velocities which do not satisfy this inequality, it is necessary to use values of  $M$  larger than  $mg/\bar{m}$ . However the positivity of  $|\gamma(\dot{x}, t)|$  can no longer be guaranteed locally around any reference velocity. In this case, instead of choosing  $\gamma_d = \gamma_g$ , one might as well set  $\gamma_d = 0$ , so that  $\gamma = \overline{\text{sat}}_M(\gamma_e) = \overline{\text{sat}}_M(\gamma_g + \gamma_{ae})$ . With this choice, the positivity of  $|\gamma(\dot{x}, t)|$  is not unconditional, but it is satisfied in the neighborhood of any reference velocity such that

$$\dot{x}_r \neq \sqrt{mg/(\bar{m}c_a)} e_3 \quad (34)$$

From Theorem 1 *local* asymptotic stability is also obtained if  $M \geq g + c_a \bar{\mathbf{v}}_{\mathbf{r}}^2$ .

**Remark 1** *The controllers of Propositions 3-5 can be modified in a similar way. Consider for example the position control law of Section 3.4. One can define (compare with (21))*

$$\gamma := \gamma_d + \overline{\text{sat}}_M(\hat{\gamma}_{e,d}) - \ddot{x}_r + h(|y|^2)y + \ddot{z}$$

with

$$\hat{\gamma}_{e,d} := \hat{\gamma}_e - \gamma_d$$

and state stability results as in Theorem 1. The sole modification concerns the condition  $M > \bar{c}_1 + \bar{c}_2(\kappa(\bar{c}_i, \bar{\mathbf{v}}_r))^2$  of Theorem 1 which yields global asymptotic stability. It has to be replaced by the stronger condition  $M > \bar{c}_1 + \bar{c}_2(\kappa(\bar{c}_i, \bar{\mathbf{v}}_r + 2\eta_z))^2$ .

## 5 Simulation results

This section illustrates the performance and robustness of the proposed controllers for a model of a VTOL vehicle similar to the “HoverEye” developed by Bertin Technologies Group (see [5, 6, 23, 24]). This vehicle, whose shape roughly corresponds to the one depicted on Figure 1, belongs to the class of “sit on tail” VTOL UAVs. It is symmetric along a privileged axis taken as the axis  $\{G; \vec{k}\}$ . In the first approximation, its inertia matrix  $J$  is diagonal and  $J \approx \text{diag}(J_1, J_1, J_2)$ .

The system’s equations used in simulations are given by (see [24] for details)

$$\left\{ \begin{array}{l} (\Sigma_1) : \begin{pmatrix} \dot{x} \\ \dot{v} \\ \dot{R} \end{pmatrix} = \begin{pmatrix} Rv \\ -S(\omega)v - ue_3 + gR^T e_3 + \frac{1}{m}R^T F_{ae} - \frac{1}{mL}S(e_3)\Gamma \\ RS(\omega) \end{pmatrix} \\ (\Sigma_2) : J\dot{\omega} = -S(\omega)J\omega + \Gamma + M_{ae} \end{array} \right. \quad (35)$$

with

- $F_{ae}$  the vector of coordinates of  $\vec{F}_{ae}$  expressed in the basis of the inertial frame  $\mathcal{I}$ , with  $\vec{F}_{ae}$  the sum of all aerodynamic reaction forces (lift, drag, momentum drag),
- $M_{ae}$  the external torque induced by these forces,
- $L$  the distance between the plane of controlled fins and the vehicle’s center of mass.

Expressions of  $F_{ae}$  and  $M_{ae}$  are specified in Appendix A.11. Wind tunnel measurements and aerodynamic modeling for this class of VTOL vehicles have been reported in [23]. By setting

$$\gamma_e := ge_3 + \frac{1}{m}F_{ae} - \frac{1}{mL}RS(e_3)\Gamma \quad (36)$$

the subsystem  $(\Sigma_1)$  in (35) takes the form of System (5). However, Assumption 1 is violated because  $F_{ae}$  depends on the vehicle’s orientation and angular velocity, and also because  $\Gamma$  is



related to the angular acceleration so that  $\gamma_e$  depends also on these variables. Discrepancies like this one between the ideal model used for the control design and the physical system represent an opportunity to test by simulation the robustness of the proposed controllers. The complete vehicle's situation (i.e.  $x$  and  $R$ ) is measured together with all velocity components (i.e.  $v$  and  $\omega$ ). The simulation results presented next have been obtained with the estimated physical parameters of the vehicle given in Table 1.

Parameter	Value	Unit
m	3	kg
g	9.8	$ms^{-2}$
$J_1$	0.1	$kgm^2$
$J_2$	0.03	$kgm^2$
L	0.2	m

Table 1: Parameters of the vehicle.

To test the robustness of the proposed controllers w.r.t. static modeling errors, we assume that the real gravity acceleration is  $g^* = 9.81 ms^{-2}$ , the real vehicle's mass is  $m^* = 3.2 kg$ , and the real vehicle's inertia matrix is  $J^* = diag(0.13, 0.13, 0.04)$ .

Among the three control modes considered in the paper, position stabilization is the most advanced one and simulations are only presented for this mode. For the first subsystem  $\Sigma_1$  the controller of Proposition 5, modified as proposed in Section 4, is applied. The desired yaw angular velocity is set to zero  $\omega_{d,3} = 0$ , and a high gain controller is applied to the second subsystem  $\Sigma_2$  in order to stabilize the angular velocity at the desired value  $\omega_d$  whose first two components are generated by the first controller. Note that the choice of a high gain controller is here justified by the fact that  $M_{ae}$  is neither measured nor estimated. The applied control torque is calculated according to

$$\Gamma = S(\omega)J\omega_d - JK_\omega(\omega - \omega_d) \quad (37)$$

with  $K_\omega$  a positive symmetric gain matrix here chosen diagonal.

The following gains and functions are used

- $k_1 = 0.24, k_2 = 0.08, k_3 = 12.8,$   
 $K_\omega = diag(20; 20; 20),$
- $h(s) = \frac{\beta}{\sqrt{1+\beta^2 s/\eta^2}}$  with  $\beta = 1.28$  and  $\eta = 12,$
- $\sigma(s) = \frac{\alpha}{k_1} \tanh\left(\frac{k_1 s}{\alpha}\right)$  with  $\alpha = 0.9,$
- $k_z = 0.8, h_z(s) = \frac{\beta_z}{\sqrt{1+\beta_z^2 s/\eta_z^2}}$  with  $\beta_z = 0.8$  and  $\eta_z = 0.8,$
- $\text{sat}_\Delta$  as given by (18) with  $\Delta = 8,$
- $\gamma_d = 0, \overline{\text{sat}}_M$  as given by (28) with  $M = 50.$

- $\mu_\tau$  as given by (24) with  $\tau = 1$ .

The gains  $k_1, k_2, k_3, h(0), k_z, h_z(0)$  have been determined via a pole placement procedure performed on the linearized system of System (9)–System (17) at the equilibrium ( $z = 0, \dot{z} = 0, \tilde{x} = 0, \tilde{v} = 0, R = I$ ) in the particular case of a reference trajectory consisting of a fixed point, with all external forces being neglected. Details of this gain tuning procedure are given in Appendix A.10. Two simulation cases are reported.

**Simulation 1: stabilization of the VTOL vehicle at a stationary point.**

The control objective is to stabilize the vehicle’s center of mass  $G$ , initially resting at the position  $x(0) = (8, 5, -8)^T$ . The initial vehicle’s attitude is given by  $R(0) = I_3$ . This corresponds to the equilibrium attitude associated with a fixed desired position in the absence of wind. The desired position is  $x_r = (0, 0, 0)^T$ . Initially, there is no wind, but a horizontal wind step velocity  $\dot{x}_f = (4, 0, 0)^T$  is introduced between the time-instants 30 s and 70 s, followed by a larger one ( $\dot{x}_f = (8, 0, 0)^T$ ) thereafter. This simulation was devised to test the robustness of the proposed controller when neither measurement nor estimation of aerodynamic reaction forces is available. To this purpose, we have used  $\hat{\gamma}_e = ge_3$  in the control calculation, whereas the real value of  $\gamma_e$  is given by (36) with  $g = g^*$  and  $m = m^*$ . It matters also to illustrate the role and importance of the integrator defined by (17). In this respect, two control versions are used for comparison purposes. The first one does not incorporate a position integral action. This corresponds to setting the terms  $z, \dot{z}, \ddot{z}$  equal to zero. The second one contains the integral action resulting from the calculation of  $z$  and its first and second order time-derivatives from (17). The evolution of the vehicle’s position and attitude is shown on Figures 2 and 3. With both control versions, the position of the vehicle’s center of mass  $G$  converges to a fixed position. However, in the no-integral action case (see Figure 2), the position error does not converge to zero, due to estimation errors on the vehicle’s physical parameters and poorly modeled aerodynamic reaction forces. Figure 3 shows that the incorporation of the proposed integral action makes this error converge to zero. Note that Assumption *iv*) of Proposition 5 ( $\lim_{s \rightarrow +\infty} h(s^2)s > |c|$ , with  $c = \hat{\gamma}_e - \gamma_e$ ) must be satisfied to guarantee the stability of the controlled system and compensate for large wind-induced perturbations. When  $\eta$ , the upper-bound of  $h(s^2)s$ , is smaller than 10 and the wind velocity is “strong” ( $\dot{x}_f = 8e_1$ ) –i.e. when modeling errors on external forces are very large– we have observed in simulation the divergence of the position error despite the integral action. This explains the use of a larger value of  $\eta$  (i.e.  $\eta = 12$ ) in the reported simulations. Recall however that, as discussed in Subsection 3.3, using a large value of  $\eta$  has the side drawback of increasing the risk of getting  $\gamma$  close to zero. It also contributes to increase the size of  $\gamma$  defined by (21), and thus also the amplitude of the control inputs defined by (22). This in turn increases the risk of saturating the actuators, with known associated destabilizing effects. To comply with actuators power limitations, a small value of  $\eta$  is preferable, and this in turn militates in favor of the on-line measurement or estimation of the apparent acceleration  $\gamma_e$ . In [13] a high gain observer of this force based on the measurement of the vehicle’s translational velocity  $\dot{x}$  and orientation  $R$ , and the thrust intensity  $T$  is proposed. Figure 4 shows simulation results of the controller with integral correction, when using such

an observer. Smaller values of  $\eta$  and  $\Delta$  –the value associated with the function  $\text{sat}_{\Delta}$ – (i.e.  $\eta = 6$ ,  $\Delta = 1$ ) are also applied. The better tracking performance of this controller, which is also used in the next simulation case, shown the interest of complementing the integral correction action with the estimation of the apparent acceleration.

**Simulation 2: Trajectory tracking with strong variable wind, large initial position error, and on-line estimation of aerodynamic forces.**

The control objective is to track the following reference trajectory

$$x_r(t) = (10 \cos(\pi t/10), 10 \sin(\pi t/10), -t)^T$$

The initial vehicle’s position and attitude are given by  $x(0) = (45, 50, -10)^T$  and  $R(0) = I_3$  respectively. Integral correction in position is used. To test the robustness of the controller w.r.t. aerodynamic perturbations, a “strong” variable wind is simulated with velocity intensity variations represented on Figure 5. Actual and estimated apparent accelerations are shown on Figure 6. Limitations of the actuators are also taken into account by saturating the applied thrust force and torque components according to the following inequality constraints

$$0 \leq T \leq 1.8m^*g^* = 56.5, \quad |\Gamma_{i=1,2,3}| \leq 0.3TL$$

The control results of Figure 7 illustrate the robustness of the controller w.r.t. strong and rapidly varying wind-induced perturbations and modeling errors. The tracking position errors decrease almost linearly from large initial values and remain small thereafter (see Figure 7.c). At the beginning of the simulation, due to the small value of  $\eta$  (i.e.  $\eta = 6$ ), the thrust input remains unsaturated (see Figure 7.e) despite large initial position errors. The saturation occurring later on during short time intervals, as a consequence of strong wind-gusts, little affects the overall tracking performance.

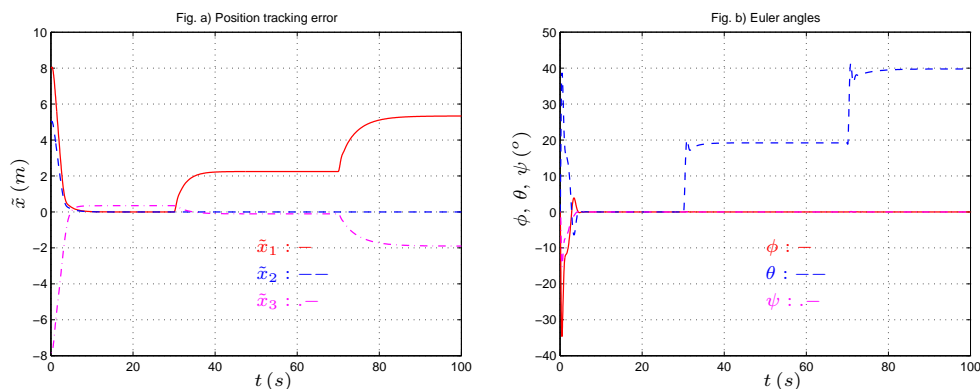


Figure 2: Vehicle's position and attitude vs. time. Fixed desired position. No integral correction and  $\eta = 12$ .

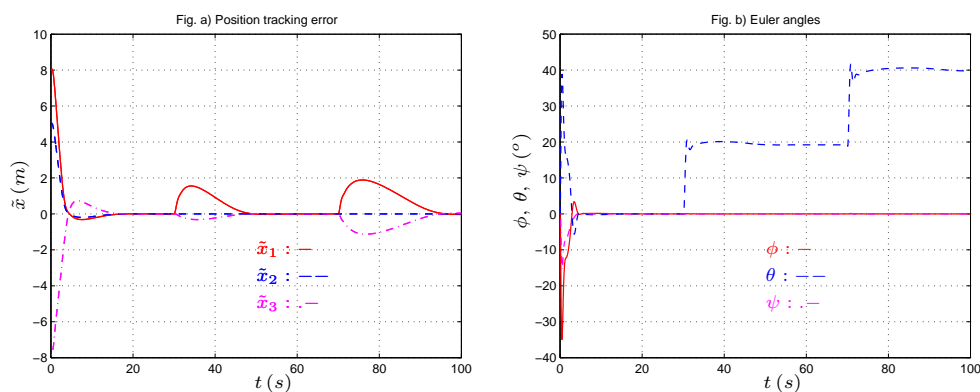


Figure 3: Vehicle's position and attitude vs. time. Fixed desired position. With integral correction,  $\eta = 12$ , and  $\Delta = 8$ .

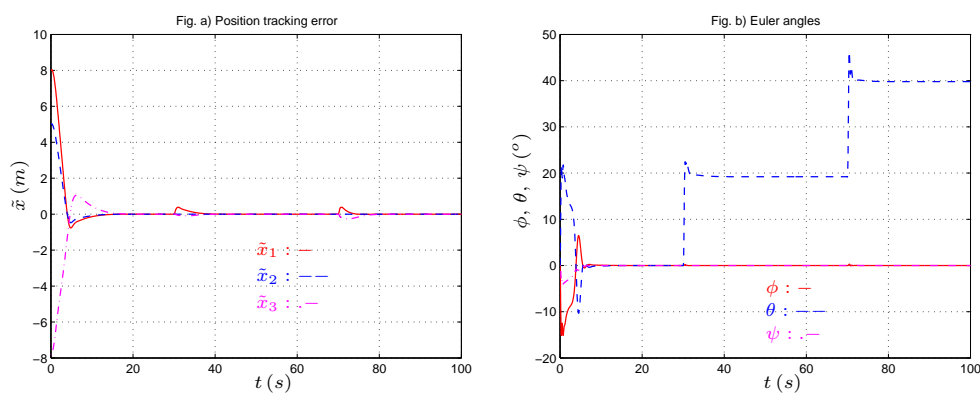


Figure 4: Vehicle's position and attitude vs. time. Fixed desired position. With integral correction,  $\eta = 6$ , and  $\Delta = 1$ . With on-line estimation of aerodynamic forces.

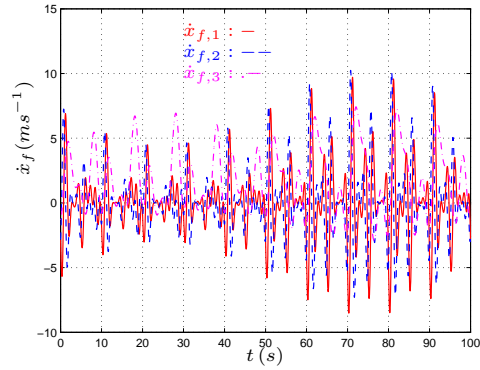
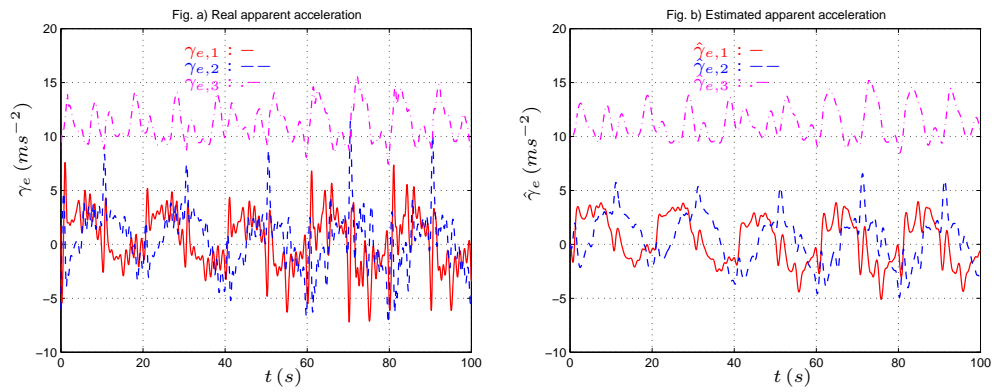


Figure 5: Wind velocities vs. time.

Figure 6: Real ( $\gamma_e$ ) and estimated ( $\hat{\gamma}_e$ ) apparent accelerations.

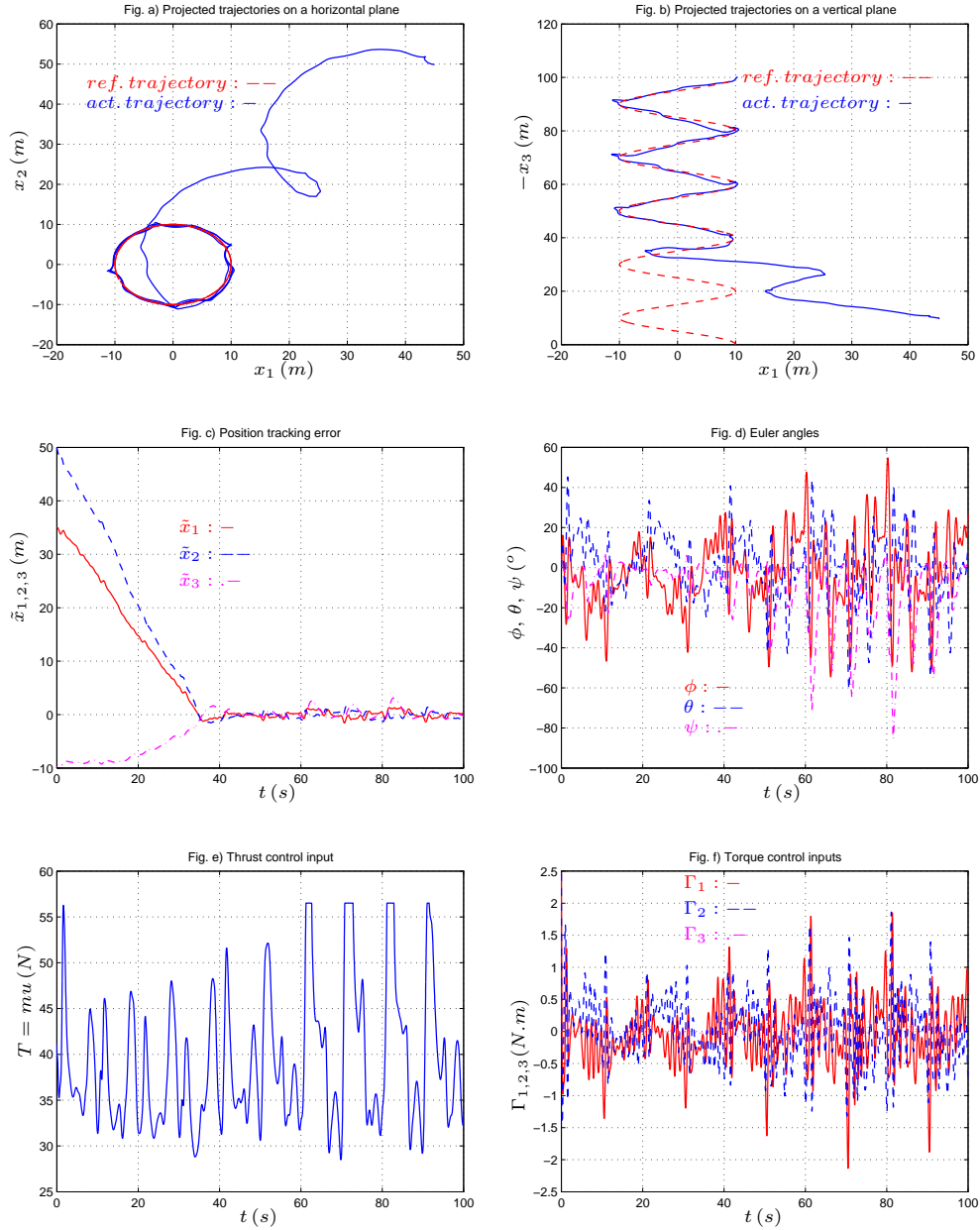


Figure 7: Ascending reference spiral and vehicle's trajectory in the presence of strong variable wind and large initial position errors. Control with integral correction,  $\eta = 6$ ,  $\Delta = 1$ , and on-line estimation of  $\gamma_e$ .

## 6 Conclusions

This paper is an attempt to set the foundations of a general approach to the control of a large family of thrust-propelled underactuated vehicles. Developing a control theory for vehicles seemingly as different as an ocean ship and a space rocket may, at first glance, appear far-fetched and unrealistic. However, a closer look at the unifying model equations of these systems brings evidence that the idea is technically relevant. The initial stage of this work logically focused on gathering information from the existing related literature and extracting the elements, at the modeling and control levels, on which a reasonably sound theory could be worked out. Among them, the basic principle according to which the thrust direction has to be monitored in order to allow for the compensation of the resultant of external forces has been the leading guide. Control laws conceived for incrementally complex objectives, ranging from joystick-augmented-control of the vehicle's attitude to autonomous trajectory tracking, have been derived with the support of rigorous Lyapunov stability and convergence analyses. The unavoidability of imprecise modeling and/or measurement of the effects of the environment on the vehicle's dynamics yields the necessity of effective integral and antiwindup correction terms, whereas this type of correction is often overlooked in many nonlinear control studies. On the other hand, the concern of genericity and generality induced a certain number of simplifying assumptions. For instance, the existence of attitude control actuators enough powerful to overcome environmental perturbing torques was assumed. Deriving an approach as little dependent as possible on vehicle particularities goes with the decoupling of the control architecture into inner hardware-dependent and outer control loops. The study focused on the latter one, and the availability of low-level servo mechanisms in charge of effectively producing the desired thrust force intensity and angular velocities –the determination of which constitutes the core of the proposed results– was not discussed or, equivalently, was assumed. Another important assumption concerns the availability of sensors providing on-line measurements of the vehicle's pose (position+attitude) and of the corresponding velocity components. Depending on the vehicles and their domains of operation, this measurement/estimation requirement can be critical. Clearly each of these simplifying assumptions needs to be re-evaluated when considering an application on a physical system. They constitute complementary research topics for existing and future developments. We also envision two important extensions to this study. The first one concerns the assumption according to which environmental drag forces only depend on the vehicle's velocity. It is necessary to relax this assumption for a number of vehicles –aeroplanes submitted to lift forces depending on the angle of attack, for instance. The other one concerns the possibility of removing the assumption of non zero-crossing upon the so-called “apparent acceleration” –the resultant of external forces and desired accelerations– via more involved, non-classical, control techniques aiming at the unconditional practical stability of the system [19]. Besides these conceptual developments, conducting experiments on physical systems, such as the VTOL “HoverEye” developed by Bertin Technologies Group, is indispensable to consolidate the results of this study, with respect to claims of robustness and performance in particular.

## References

- [1] M.J. Abzug and E.E. Larrabee. *Airplane Stability and Control*. Cambridge University Press, second edition, 2002.
- [2] J.R. Azinheira, A. Moutinho, and E.C. De Paiva. Airship hover stabilization using a backstepping control approach. *Journal of Guidance, Control, and Dynamics*, 29(4):903–914, 2006.
- [3] S. Bertrand, T. Hamel, and H. Piet-Lahanier. Stabilization of a small unmanned aerial vehicle model without velocity measurement. In *IEEE Conf. on Robotics and Automation*, pages 724– 729, 2007.
- [4] R.P. Boas, Jr., and M.B. Marcus. Inverse functions and integration by parts. *The American Mathematical Monthly*, 81(7):760–761, 1974.
- [5] F. Le Bras, T. Hamel, and R. Mahony. Visual servoring of a vtol vehicle using virtual states. In *IEEE Conf. on Decision and Control*, pages 6442–6447, 2007.
- [6] F. Le Bras, R. Mahony, T. Hamel, and P. Binetti. Adaptive filtering and image based visual servo control of a ducted fan flying robot. In *IEEE Conf. on Decision and Control*, pages 1751– 1757, 2006.
- [7] B. Etkin and L.D. Reid. *Dynamics of Flight: Stability and Control*. John Wiley and Sons, third edition, 1996.
- [8] T.I. Fossen. *Guidance and control of ocean vehicles*. Wiley, 1994.
- [9] E. Frazzoli, M. Dahleh M. A., and E. Feron. Real-time motion planning for agile autonomous vehicles. *AIAA Journal of Guidance Control and Dynamics*, 25(1):116–129, 2002.
- [10] R. Freeman and L. Praly. Integrator backstepping for bounded controls and control rates. *IEEE Trans. on Automatic Control*, 43(2):258–262, 1998.
- [11] T. Hamel, R. Mahony, R. Lozano, and J. Ostrowski. Dynamic modelling and configuration stabilization for an x4-flyer. In *IFAC World Congress*, pages 200–212, 2002.
- [12] J. Hauser, S. Sastry, and G. Meyer. Nonlinear control design for slightly non-minimum phase systems: Application to v/stol. *Automatica*, 28:651–670, 1992.
- [13] M.-D. Hua, P. Morin, and C. Samson. Balanced-force-control for underactuated thrust-propelled vehicles. In *IEEE Conf. on Decision and Control*, pages 6435–6441, 2007.
- [14] A. Isidori, L. Marconi, and A. Serrani. *Robust autonomous guidance : an internal model approach*. Advances in industrial control. Springer Verlag, 2003.
- [15] H.K. Khalil. *Nonlinear systems*. Prentice Hall, third edition, 2002.



- 
- [16] L. Lipera, J. Colbourne, M. Tischler, M. Mansur, M. Rotkowitz, and P. Patangui. The micro craft istar micro-air vehicle: Control system design and testing. In *Annual Forum of the American Helicopter Society*, pages 1–11, 2001.
- [17] L. Marconi, A. Isidori, and A. Serrani. Autonomous vertical landing on an oscillating platform: an internal-model based approach. *Automatica*, 38:21–32, 2002.
- [18] A. Micaelli and C. Samson. Trajectory tracking for unicycle-type and two-steering-wheels mobile robots. Technical Report 2097, INRIA, 2001. Available at <http://www-sop.inria.fr/rapports/sophia/RR-2097.html>.
- [19] P. Morin and C. Samson. Control with transverse functions and a single generator of underactuated mechanical systems. In *IEEE Conf. on Decision and Control*, pages 6110–6115, 2006.
- [20] A. Moutinho and J.R. Azinheira. Stability and robustness analysis of the aurora airship control system using dynamic inversion. In *IEEE Conf. on Robotics and Automation*, pages 2265–2270, 2005.
- [21] R. Olfati-Saber. Global configuration stabilization for the vtol aircraft with strong input coupling. *IEEE Trans. on Automatic Control*, 47:1949–1952, 2002.
- [22] J.-M. Pflimlin. *Commande d'un minidrone à hélice carénée: de la stabilisation dans le vent à la navigation autonome (in French)*. PhD thesis, Ecole Doctorale Systèmes de Toulouse, 2006.
- [23] J.-M. Pflimlin, P. Binetti, D. Trouchet, P. Souères, and T. Hamel. Aerodynamic modeling and practical attitude stabilization of a ducted fan uav. In *European Control Conference*, pages 4023–4029, 2007.
- [24] J.-M. Pflimlin, P. Souères, and T. Hamel. Position control of a ducted fan vtol uav in crosswind. *International Journal of Control*, 80(5):666–683, 2007.
- [25] R.W. Prouty. *Helicopter Performance, Stability, and Control*. Krieger, 1986.
- [26] J.E. Refsnes, K.Y. Pettersen, and A.J. Sørensen. Control of slender body underactuated auvs with current estimation. In *IEEE Conf. on Decision and Control*, pages 43–50, 2006.
- [27] S. Saripalli, J.F. Montgomery, and G.S. Sukhatme. Vision based autonomous landing of an unmanned aerial vehicle. In *IEEE Conf. on Robotics and Automation*, pages 2799–2804, 2002.
- [28] R. Sepulchre, M. Janković, and P. Kokotović. *Constructive Nonlinear Control*. Springer-Verlag, 1997.

- [29] O. Shakernia, Y. Ma, T. Koo, and S. Sastry. Landing an unmanned air vehicle: Vision based motion estimation and nonlinear control. *Asian Journal of Control*, 1(3):128–145, 1999.
- [30] A. Tayebi and S. McGilvray. Attitude stabilization of a vtol quadrotor aircraft. *IEEE Trans. on Control Systems Technology*, 14(3):562–571, 2006.
- [31] A.R. Teel. Global stabilization and restricted tracking for multiple integrators with bounded controls. *Systems & Control Letters*, 18:165–171, 1992.
- [32] H. Yoon and P. Tsiotras. Singularity analysis of variable-speed control moment gyros. *Journal of Guidance, Control, and Dynamics*, 27(3):374–386, 2004.

## A Appendix

### A.1 Proof of Proposition 1

Consider the following candidate Lyapunov function

$$V = 1 - \bar{\gamma}_3 = 1 - \cos \tilde{\theta} \quad (38)$$

Differentiating  $V$  along the solutions of the system  $\dot{R} = RS(\omega)$  and using Lemma 2 with  $|\gamma| = 1$  (see Appendix A.8), one has

$$\dot{V} = (\bar{\gamma}_1 \quad \bar{\gamma}_2) \left[ \begin{pmatrix} -\omega_2 \\ \omega_1 \end{pmatrix} + \begin{pmatrix} -\gamma^T S(Re_2) \dot{\gamma} \\ \gamma^T S(Re_1) \dot{\gamma} \end{pmatrix} \right]$$

Substituting expressions (7) of  $\omega_1$ ,  $\omega_2$  and using (40), one gets

$$\dot{V} = -k \frac{\bar{\gamma}_1^2 + \bar{\gamma}_2^2}{(1 + \bar{\gamma}_3)^2} = -k \frac{1 - \bar{\gamma}_3}{1 + \bar{\gamma}_3} = -\frac{kV}{1 + \bar{\gamma}_3} \leq -\frac{kV}{2} \leq 0 \quad (39)$$

This relation points out that  $V$  converges exponentially to zero which also implies the exponential convergence of  $\tilde{\theta}$  to zero. As for the stability of the equilibrium  $\tilde{\theta} = 0$ , it is a direct consequence of (38) and (39).

### A.2 Proof of Proposition 2

It follows from the definition of  $\tilde{\theta}$  that

$$\tan^2(\tilde{\theta}/2) = \frac{\bar{\gamma}_1^2 + \bar{\gamma}_2^2}{(|\gamma| + \bar{\gamma}_3)^2} = \frac{|\gamma| - \bar{\gamma}_3}{|\gamma| + \bar{\gamma}_3} \quad (40)$$

Consider the candidate Lyapunov function  $V$  defined by (12). Differentiating  $V$  along the solutions of System (9b)-(9c) and using Lemma 2 (see Appendix A.8), one gets

$$\begin{aligned}\dot{V} &= \tilde{v}^T (-ue_3 + \bar{\gamma}) + \frac{1}{|\gamma|k_2} (\bar{\gamma}_1 \quad \bar{\gamma}_2) \left[ \begin{pmatrix} -\omega_2 \\ \omega_1 \end{pmatrix} + \frac{1}{|\gamma|^2} \begin{pmatrix} -\gamma^T S(Re_2)\dot{\gamma} \\ \gamma^T S(Re_1)\dot{\gamma} \end{pmatrix} \right] \\ &= \tilde{v}_3 (-u + \bar{\gamma}_3) + \frac{1}{|\gamma|k_2} (\bar{\gamma}_1 \quad \bar{\gamma}_2) \left[ \begin{pmatrix} -\omega_2 \\ \omega_1 \end{pmatrix} + \frac{1}{|\gamma|^2} \begin{pmatrix} -\gamma^T S(Re_2)\dot{\gamma} \\ \gamma^T S(Re_1)\dot{\gamma} \end{pmatrix} + |\gamma|k_2 \begin{pmatrix} \tilde{v}_1 \\ \tilde{v}_2 \end{pmatrix} \right]\end{aligned}$$

Substituting expressions (11) of  $u$ ,  $\omega_1$ ,  $\omega_2$  and using (40), one obtains

$$\dot{V} = -|\gamma|k_1\tilde{v}_3^2 - \frac{k_3}{k_2} \frac{\bar{\gamma}_1^2 + \bar{\gamma}_2^2}{(|\gamma| + \bar{\gamma}_3)^2} = -|\gamma|k_1\tilde{v}_3^2 - \frac{k_3}{k_2} \tan^2(\tilde{\theta}/2) \quad (41)$$

The Lyapunov function derivative is negative semi-definite, so that the velocity error term  $\tilde{v}$  is bounded. The next step of the proof consists in showing that  $\dot{V}$  is uniformly continuous along each system's solution in order to deduce, by application of Barbalat's lemma (see [15]), the convergence of  $\tilde{v}_3$  and  $\tilde{\theta}$  to zero<sup>2</sup>. To this purpose, it suffices to show that  $\dot{V}$  is bounded. In view of (41), Assumption 5, and the boundedness of  $\tilde{v}$ , this condition is satisfied if  $\gamma$ ,  $\dot{\gamma}$ ,  $\tilde{v}_3$ , and  $\frac{d}{dt} \tan^2(\tilde{\theta}/2)$  are bounded.

From Assumption 4, the boundedness of  $\tilde{v}$ , and the relation  $\tilde{v} = R^T(\dot{x} - \dot{x}_r)$ , it follows that  $\dot{x}$  is bounded. Therefore, using Assumptions 1 and 4, one deduces that  $\gamma_e$ ,  $\gamma$  and  $\bar{\gamma}$  are also bounded, and that  $u$  (given by (11)) is also well-defined and bounded. This implies that  $\ddot{x}$  given by

$$\ddot{x} = -uRe_3 + \gamma_e(\dot{x}, t) \quad (42)$$

is bounded. Since

$$\dot{\gamma}_e(\dot{x}, t) = \frac{\partial \gamma_e}{\partial \dot{x}}(\dot{x}, t)\dot{x} + \frac{\partial \gamma_e}{\partial t}(\dot{x}, t),$$

it comes, from Assumptions 1 and 4 and the fact that  $\dot{x}$  and  $\ddot{x}$  are bounded, that  $\dot{\gamma}_e$  and  $\dot{\gamma}$  are also bounded. Let us now show that along each system's solution, there exists  $\varepsilon > 0$  such that

$$|\tilde{\theta}(t)| \leq \pi - \varepsilon, \quad \forall t \quad (43)$$

It follows from (11), (40), and Lemma 2 that

$$\frac{d}{dt}(1 - \cos \tilde{\theta}) = -k_2(\bar{\gamma}_1\tilde{v}_1 + \bar{\gamma}_2\tilde{v}_2) - k_3 \frac{|\gamma| - \bar{\gamma}_3}{|\gamma| + \bar{\gamma}_3} = -k_2(\bar{\gamma}_1\tilde{v}_1 + \bar{\gamma}_2\tilde{v}_2) - k_3 \tan^2(\tilde{\theta}/2) \quad (44)$$

Since  $\bar{\gamma}$  and  $\tilde{v}$  are bounded, one can ensure that there exists  $\varepsilon_1 > 0$  such that

$$|\tilde{\theta}| > \pi - \varepsilon_1 \implies \frac{d}{dt}(1 - \cos \tilde{\theta}) < 0$$

Equation (43) is thus satisfied with  $\varepsilon = \min\{\varepsilon_1, \pi - |\tilde{\theta}(0)|\}$  ( $> 0$ ). This implies the boundedness of  $\tan(\tilde{\theta}/2)$  and also, from (40), of  $1/(|\gamma| + \bar{\gamma}_3)$ . Along with Assumption 5 and the fact

<sup>2</sup>Note that LaSalle's theorem does not apply since the closed-loop dynamics is not autonomous.

that  $\tilde{v}$ ,  $\gamma$ ,  $\bar{\gamma}$ ,  $\dot{\gamma}$  are bounded, this ensures that the control inputs  $\omega_1$  and  $\omega_2$ , and thus  $\omega$ , are well-defined and bounded. Since  $\gamma$ ,  $\tilde{v}$ ,  $\omega$ ,  $u$  are bounded, it follows from (9b) that  $\dot{\tilde{v}}$  is also bounded. Finally, since both  $\dot{\gamma}$  and  $\omega$  are bounded, one deduces that  $\dot{\tilde{\gamma}}$  is bounded. The boundedness of  $\frac{d}{dt} \tan^2(\tilde{\theta}/2)$  then follows from (40) and from the boundedness of  $1/(|\gamma| + \gamma_3)$ . This concludes the proof of uniform continuity of  $\dot{V}$  and of the convergence of  $\tilde{v}_3$  and  $\tilde{\theta}$  to zero. Note from (40) that  $\bar{\gamma}_1$  and  $\bar{\gamma}_2$  also converge to zero.

There remains to show that  $\tilde{v}_1$  and  $\tilde{v}_2$  converge to zero. Let  $\bar{\gamma}_{1,2}$  denote the vector  $(\bar{\gamma}_1, \bar{\gamma}_2)^T$ . By a direct calculation, one deduces from Lemma 2 and (11) that

$$\frac{d}{dt} \frac{\bar{\gamma}_{1,2}}{|\gamma|} = a(t) + b(t) \quad (45)$$

with

$$a(t) := \bar{\gamma}_3 \begin{pmatrix} -k_2 \tilde{v}_1 - \frac{k_3 \bar{\gamma}_1}{(|\gamma| + \bar{\gamma}_3)^2} \\ -k_2 \tilde{v}_2 - \frac{k_3 \bar{\gamma}_2}{(|\gamma| + \bar{\gamma}_3)^2} \end{pmatrix}, \quad b(t) := \frac{1}{|\gamma|} \left( \omega_3 + \frac{1}{|\gamma|^2} \gamma^T S(Re_3) \dot{\gamma} \right) \begin{pmatrix} \bar{\gamma}_2 \\ -\bar{\gamma}_1 \end{pmatrix}$$

It is straightforward to verify that  $\dot{a}(t)$  is bounded (so that  $a(t)$  is uniformly continuous) based on the boundedness of  $\dot{\tilde{v}}$ ,  $\bar{\gamma}$ ,  $\dot{\tilde{\gamma}}$ , and  $1/(|\gamma| + \bar{\gamma}_3)$ . Because  $b(t)$  is not necessarily uniformly continuous (because of the terms  $\omega_3$  and  $\dot{\gamma}$ ), the classical version of Barbalat's lemma does not apply. This explains the use of the slightly generalized version given by Lemma 3 (see Appendix A.9). Using the boundedness of  $\omega_3$ , Assumption 5, and the properties obtained previously (i.e. convergence of  $\bar{\gamma}_{1,2}$  to zero and boundedness of  $\dot{\gamma}$ ), one verifies that  $b(t)$  converges to zero. Direct application of Lemma 3 to System (45) ensures the convergence of  $\frac{d}{dt} \frac{\bar{\gamma}_{1,2}}{|\gamma|}$  to zero. Since  $\bar{\gamma}_{1,2}$  converges to zero and  $|\gamma| + \bar{\gamma}_3 > 0$ , the convergence of  $\tilde{v}_1, \tilde{v}_2$  to zero follows.

As for the stability of the equilibrium  $(\tilde{v}, \tilde{\theta}) = (0, 0)$ , it is a direct consequence of (12) and (41).

### A.3 Proof of Proposition 3

From the definition of  $\gamma$  given by (16), equation (9b) can be rewritten as

$$\dot{\tilde{v}} = -S(\omega) \tilde{v} - ue_3 + R^T \gamma - R^T h(|I_v|^2) I_v + R^T c \quad (46)$$

Define  $f : s \mapsto h(s^2)s$  and  $f^{-1}$  as its inverse function. Note, from (15), that  $f$  is a strictly increasing continuous function. Since  $h$  is strictly positive, one has  $f(0) = 0$ . Therefore, the use of Young's inequality (see [4]) allows to establish the following relation

$$c^T I_v \leq |c| |I_v| \leq \int_0^{|I_v|} f(s) ds + \int_0^{|c|} f^{-1}(s) ds$$

This leads us to consider the following candidate Lyapunov function  $V$  defined by

$$V = \frac{1}{2} \tilde{v}^T \tilde{v} + \frac{1}{k_2} \left( 1 - \frac{\tilde{\gamma}_3}{|\gamma|} \right) + \int_0^{|\tilde{I}_v|} f(s) ds - c^T I_v + \int_0^{|c|} f^{-1}(s) ds \quad (47)$$

It is straightforward to verify that the function  $V$  is positive and proper w.r.t.  $\tilde{v}$ . One verifies also that  $V$  is proper w.r.t.  $I_v$  by verifying that the Hessian matrix of  $V$  w.r.t.  $I_v$  is definite positive, i.e.  $\frac{\partial^2 V}{\partial I_v^2} > 0$ , using the condition (15) of the function  $h$ . Using (46), Lemma 2, and the relation  $\dot{I}_v = R\tilde{v}$ , one gets

$$\dot{V} = \tilde{v}^T (-ue_3 + \tilde{\gamma}) + \frac{1}{|\gamma|k_2} (\tilde{\gamma}_1 \quad \tilde{\gamma}_2) \left[ \begin{pmatrix} -\omega_2 \\ \omega_1 \end{pmatrix} + \frac{1}{|\gamma|^2} \begin{pmatrix} -\gamma^T S(Re_2) \dot{\gamma} \\ \gamma^T S(Re_1) \dot{\gamma} \end{pmatrix} \right] \quad (48)$$

Substituting the control expression (11) into (48), one obtains

$$\dot{V} = -|\gamma|k_1 \tilde{v}_3^2 - \frac{k_3}{k_2} \frac{\tilde{\gamma}_1^2 + \tilde{\gamma}_2^2}{(|\gamma| + \tilde{\gamma}_3)^2} \quad (49)$$

Then, the proof of convergence of  $(I_v, \tilde{v}, \tilde{\theta})$  to  $(I_v^*, 0, 0)$  proceeds as for Proposition 2. Note in particular that the condition (15) of the function  $h$  is useful to ensure the boundedness of  $\dot{\gamma}$ , and its combination with Assumption *iii*) of Proposition 3 implies the existence of a unique vector  $I_v^*$  such that  $h(|I_v^*|^2)I_v^* = c$ . Furthermore, to prove that  $I_v$  converges to  $I_v^*$  one can apply Barbalat's lemma given in Appendix A.9 to (46) with

$$a(t) := -R^T h(|I_v|^2)I_v + R^T c, \quad b(t) := -S(\omega)\tilde{v} - ue_3 + R^T \gamma$$

As for the stability of the equilibrium point  $(I_v, \tilde{v}, \tilde{\theta}) = (I_v^*, 0, 0)$ , it is a direct consequence of (47), (49), and the fact that this point is the unique minimum of the function  $V$ .

#### A.4 Proof of Proposition 4

From (9b) and (20), it follows that the time-derivative of  $\bar{v}$  satisfies the following equation

$$\dot{\bar{v}} = -S(\omega)\bar{v} - ue_3 + R^T \ddot{z} + R^T (\gamma_e - \ddot{x}_r)$$

which can be rewritten as

$$\dot{\bar{v}} = -S(\omega)\bar{v} - ue_3 - R^T h(|y|^2)y + R^T \gamma + R^T c \quad (50)$$

with  $\gamma$  defined by (21). Consider the candidate Lyapunov function

$$V = \frac{1}{2} \bar{v}^T \bar{v} + \frac{1}{k_2} \left( 1 - \frac{\tilde{\gamma}_3}{|\gamma|} \right) + \int_0^{|\bar{y}|} f(s) ds - c^T y + \int_0^{|c|} f^{-1}(s) ds \quad (51)$$

where the definition of  $f$  is given in the proof of Proposition 3 and  $\bar{\gamma}$  is given by (6). Analogously to the proof of Proposition 3, one verifies that  $V$  is positive and proper w.r.t.  $\tilde{v}$  and  $y$ . Using (50), (22), and the relation  $\dot{y} = R\tilde{v}$ , one gets

$$\dot{V} = -|\gamma|k_1\tilde{v}_3^2 - \frac{k_3}{k_2} \frac{\bar{\gamma}_1^2 + \bar{\gamma}_2^2}{(|\gamma| + \bar{\gamma}_3)^2} \quad (52)$$

From (17), one verifies that  $z$ ,  $\dot{z}$ , and  $\ddot{z}$  are bounded. From (51) and (52), one deduces that  $y$  and  $\tilde{v}$  are bounded. Since  $z$  and  $\dot{z}$  are bounded, the relations  $y = \tilde{x} + z$  and  $\tilde{v} = \tilde{v} + R^T \dot{z}$  imply that  $\tilde{x}$  and  $\tilde{v}$  are also bounded. Then it follows from Property *P1* of the function  $\text{sat}_\Delta$ , Property (15) of the function  $h_z$ , and System (17) that  $z^{(3)}$  remains bounded. Denote  $z^*$  the unique solution to  $h(|z^*|^2)z^* = c$ . From there, with the same arguments as in the proof of Proposition 3, one deduces the convergence of  $(y, \tilde{v}, \tilde{\theta})$  to  $(z^*, 0, 0)$  and the stability of this equilibrium of the  $(y, \tilde{v}, \tilde{\theta})$  subsystem.

Define

$$\begin{aligned} \bar{y} &:= y - z^*, & \bar{z} &:= z - z^*, & w &:= \dot{z}, \\ g_z(\bar{y}, \bar{z}) &:= h_z(|\bar{y} - \bar{z}|^2)(\bar{y} - \bar{z}) + h_z(|\bar{z}|^2)\bar{z} \end{aligned}$$

Note that  $g_z(\bar{y}, \bar{z})$  is bounded and vanishes ultimately since  $\bar{y}$  converges to zero. Note also that  $\tilde{x} = y - z = \bar{y} - \bar{z}$ . Then, System (17) can be rewritten as

$$\begin{cases} \dot{\bar{z}} &= w \\ \dot{w} &= -2k_z w - k_z^2 \bar{z} + k_z^2 (\text{sat}_\Delta(\bar{z} + z^*) - z^*) - k_z h_z(|\bar{z}|^2)\bar{z} + k_z g_z(\bar{y}, \bar{z}) \end{cases}$$

or in the more compact form

$$\dot{Z} = F(Z) + G(\bar{y}, Z) \quad (53)$$

with  $Z := (\bar{z}, w)^T$ ,

$$F(Z) := \begin{pmatrix} w \\ -2k_z w - k_z^2 \bar{z} + k_z^2 (\text{sat}_\Delta(\bar{z} + z^*) - z^*) - k_z h_z(|\bar{z}|^2)\bar{z} \end{pmatrix},$$

and  $G(\bar{y}, Z) := (0, k_z g_z(\bar{y}, \bar{z}))^T$  which vanishes ultimately.

One verifies that  $Z = 0$  is the globally asymptotically stable point of the system  $\dot{Z} = F(Z)$  by considering the following candidate Lyapunov function

$$U = \frac{1}{2k_z} \int_0^{|\bar{z}|^2} h_z(s) ds + \frac{1}{2} |\bar{z}|^2 + \frac{1}{2} \left| \bar{z} + \frac{w}{k_z} \right|^2 \quad (54)$$

Indeed, differentiating  $U$  along the solution of the system  $\dot{Z} = F(Z)$  and using Property *P4* of the function  $\text{sat}_\Delta$  and Assumption *iv*) of Proposition 4, one obtains

$$\begin{aligned} \dot{U} &= -h_z(|\bar{z}|^2)|\bar{z}|^2 - k_z \left( |\bar{z}|^2 + \left| \bar{z} + \frac{w}{k_z} \right|^2 - (\bar{z}^T + (\text{sat}_\Delta(\bar{z} + z^*) - z^*))^T \left( \bar{z} + \frac{w}{k_z} \right) \right) \\ &\leq -h_z(|\bar{z}|^2)|\bar{z}|^2 - k_z |\bar{z}|^2 - k_z \left| \bar{z} + \frac{w}{k_z} \right|^2 + 2k_z |\bar{z}| \left| \bar{z} + \frac{w}{k_z} \right| \end{aligned} \quad (55)$$

Since  $z$  is bounded,  $\bar{z}$  is also bounded from its definition. As a consequence, there exists  $\delta_z > 0$  such that  $h_z(|\bar{z}|^2) > \delta_z$ . This, along with (55), implies that there exist some constants  $\alpha_z, \alpha_w > 0$  such that

$$\dot{U} \leq -\alpha_z |\bar{z}|^2 - \alpha_w \left| \bar{z} + \frac{w}{k_z} \right|^2 \quad (56)$$

Applying Lyapunov's theorem one then shows that  $\bar{z}$ ,  $w$ , and thus  $U$  converge to zero. The stability of the equilibrium  $Z = 0$  of the system  $\dot{Z} = F(Z)$  results from (54) and (56).

Since  $Z = 0$  is the globally asymptotically stable point of the system  $\dot{Z} = F(Z)$ ,  $Z$  is bounded, and  $G(\bar{y}, Z)$  converges to zero, then for System (53)  $Z$  converges also to zero. So that  $(z, \dot{z})$  converges to  $(z^*, 0)$ . The convergence of  $\bar{z}$  and  $y := \bar{z} + \tilde{x}$  to zero implies that  $\tilde{x}$  converges to zero. Finally, since  $\bar{v} := \tilde{v} + R^T \dot{z}$  and  $\dot{z}$  converge to zero,  $\tilde{v}$  also converges to zero.

Let us finally establish the stability of the equilibrium point  $(z, \dot{z}, \tilde{x}, \tilde{v}, \tilde{\theta}) = (z^*, 0, 0, 0, 0)$ . From (51) and (52),  $(\bar{v}, \bar{y}, \tilde{\theta}) = (0, 0, 0)$  is a stable equilibrium of the controlled system, and from (54) and (56),  $Z = 0$  is an asymptotically stable equilibrium point of the system  $\dot{Z} = F(Z)$ . Since the function  $G$  in (53) is continuous and identically zero when  $\bar{y} = 0$ , one deduces that  $(\bar{v}, \bar{y}, \tilde{\theta}, Z) = (0, 0, 0, 0)$  is also a stable equilibrium of the controlled system. This directly implies the stability of the equilibrium  $(z, \dot{z}, \tilde{x}, \tilde{v}, \tilde{\theta}) = (z^*, 0, 0, 0, 0)$ .

## A.5 Proof of Proposition 5

The positivity of the thrust input  $u$  is easily verified from the definition of  $u$  given in (23) and the assumptions on  $\sigma$ , given in Proposition 5. Consider now the candidate Lyapunov function given by (51). Using (50) and Lemma 2 (see Appendix A.8), one gets

$$\begin{aligned} \dot{V} &= \bar{v}^T (-ue_3 + \bar{\gamma}) + \frac{1}{|\gamma|k_2} (\bar{\gamma}_1 \quad \bar{\gamma}_2) \left[ \begin{pmatrix} -\omega_2 \\ \omega_1 \end{pmatrix} + \frac{1}{|\gamma|^2} \begin{pmatrix} -\gamma^T S(Re_2) \dot{\gamma} \\ \gamma^T S(Re_1) \dot{\gamma} \end{pmatrix} \right] \\ &= \bar{v}_3 (-u + |\gamma|) - \bar{v}_3 (|\gamma| - \bar{\gamma}_3) \\ &\quad + \frac{1}{|\gamma|k_2} (\bar{\gamma}_1 \quad \bar{\gamma}_2) \left[ \begin{pmatrix} -\omega_2 \\ \omega_1 \end{pmatrix} + \frac{1}{|\gamma|^2} \begin{pmatrix} -\gamma^T S(Re_2) \dot{\gamma} \\ \gamma^T S(Re_1) \dot{\gamma} \end{pmatrix} + |\gamma|k_2 \begin{pmatrix} \bar{v}_1 \\ \bar{v}_2 \end{pmatrix} \right] \\ &= \bar{v}_3 (-u + |\gamma|) \\ &\quad + \frac{1}{|\gamma|k_2} (\bar{\gamma}_1 \quad \bar{\gamma}_2) \left[ \begin{pmatrix} -\omega_2 \\ \omega_1 \end{pmatrix} + \frac{1}{|\gamma|^2} \begin{pmatrix} -\gamma^T S(Re_2) \dot{\gamma} \\ \gamma^T S(Re_1) \dot{\gamma} \end{pmatrix} + |\gamma|k_2 \begin{pmatrix} \bar{v}_1 \\ \bar{v}_2 \end{pmatrix} - \frac{|\gamma|k_2 \bar{v}_3}{|\gamma| + \bar{\gamma}_3} \begin{pmatrix} \bar{\gamma}_1 \\ \bar{\gamma}_2 \end{pmatrix} \right] \end{aligned} \quad (57)$$

Substituting the control expression (23) into (57), one obtains

$$\dot{V} = -|\gamma|k_1 \sigma(\bar{v}_3) \bar{v}_3 - \frac{k_3}{k_2} \frac{\bar{\gamma}_1^2 + \bar{\gamma}_2^2}{(|\gamma| + \bar{\gamma}_3)^2} \quad (58)$$

From this equality, the proof of this proposition proceeds like the proof of Proposition 4.

## A.6 Proof of Proposition 6

The uniform ultimate boundedness of  $\dot{x}$  results from (26) and Assumption 3 by calculating the time-derivative of  $V = \frac{1}{2}|\dot{x}|^2$  and showing that it is negative when  $|\dot{x}|$  exceeds a certain threshold. More precisely, one has

$$\dot{V} = \dot{x}^T(-uRe_3 + \gamma_e(\dot{x}, t))$$

Using Assumption 3 and the inequality (26), one obtains

$$\begin{aligned} \dot{V} &\leq |\dot{x}||u| + \frac{c_3}{m}|\dot{x}| - \frac{c_4}{m}|\dot{x}|^3 \\ &\leq |\dot{x}| \left( \beta_1 + \left( \beta_2 + \frac{c_3}{m} \right) |\dot{x}| - \frac{c_4}{m} |\dot{x}|^2 \right) \end{aligned}$$

so that  $\dot{x}$  is u.u.b. by

$$-\frac{1}{2} \left( \beta_2 + \frac{c_3}{m} \right) + \frac{1}{2} \sqrt{\left( \beta_2 + \frac{c_3}{m} \right)^2 + \frac{4\beta_1 c_4}{m}}$$

In view of Assumption 1, the uniform ultimate boundedness of  $\gamma_e$  follows. Since  $\dot{x}$  is u.u.b., the thrust input  $u$  is also u.u.b.. Then, one deduces from (42) that  $\ddot{x}$  is u.u.b.. Combining with Assumption 1, this implies that  $\dot{\gamma}_e$  is also u.u.b..

## A.7 Proof of Theorem 1

The following technical lemma is used in the proof of Theorem 1

**Lemma 1** *Let  $\gamma_{e,d}$  as defined by (30). If  $M \geq \bar{c}_1 + \bar{c}_2(\kappa(\bar{c}_i, \bar{\mathbf{v}}_{\mathbf{r}}))^2$ , then  $\forall(\dot{x}, t)$ ,*

$$\tilde{v}^T R^T (\gamma_{e,d}(\dot{x}, t) - \overline{\text{sat}}_M(\gamma_{e,d}(\dot{x}, t))) \leq 0 \quad (59)$$

**Proof** Two cases are considered:

i) If  $|\gamma_{e,d}(\dot{x}, t)| < M$ , Property P2 of the saturation function  $\overline{\text{sat}}_M$  implies that  $\gamma_{e,d}(\dot{x}, t) = \overline{\text{sat}}_M(\gamma_{e,d}(\dot{x}, t))$ , and the result follows.

ii) If  $|\gamma_{e,d}(\dot{x}, t)| \geq M$ , it follows from (32) and the choice of  $M$  that  $|\dot{x}| > \kappa(\bar{c}_i, \bar{\mathbf{v}}_{\mathbf{r}})$ . Then, using Property P4 of the saturation function  $\overline{\text{sat}}_M$ , (32), the relations  $\phi(\gamma_{e,d}(\dot{x}, t)) \leq 1$  and  $R\tilde{v} = \dot{x} - \dot{x}_r$ , one gets

$$\begin{aligned} \tilde{v}^T R^T (\gamma_{e,d}(\dot{x}, t) - \overline{\text{sat}}_M(\gamma_{e,d}(\dot{x}, t))) &= (1 - \phi(\gamma_{e,d}(\dot{x}, t)))(\dot{x} - \dot{x}_r)^T \gamma_{e,d}(\dot{x}, t) \\ &\leq (1 - \phi(\gamma_{e,d}(\dot{x}, t)))(\dot{x} \gamma_{e,d}(\dot{x}, t) + \bar{\mathbf{v}}_{\mathbf{r}} |\gamma_{e,d}(\dot{x}, t)|) \\ &\leq -(1 - \phi(\gamma_{e,d}(\dot{x}, t)))(\bar{c}_4 |\dot{x}|^3 - \bar{c}_2 \bar{\mathbf{v}}_{\mathbf{r}} |\dot{x}|^2 - \bar{c}_3 |\dot{x}| - \bar{c}_1 \bar{\mathbf{v}}_{\mathbf{r}}) \end{aligned}$$

From the definition of the function  $\kappa$ , the inequality  $|\dot{x}| > \kappa(\bar{c}_i, \bar{\mathbf{v}}_{\mathbf{r}})$  implies

$$\bar{c}_4 |\dot{x}|^3 - \bar{c}_2 \bar{\mathbf{v}}_{\mathbf{r}} |\dot{x}|^2 - \bar{c}_3 |\dot{x}| - \bar{c}_1 \bar{\mathbf{v}}_{\mathbf{r}} \geq 0$$



Thus, inequality (59) follows.  $\blacksquare$

From (25) and (31), relation (26) holds true for some positive constants  $\beta_1, \beta_2$ . Property 2 of Theorem 1 (together with the completeness of the system's solutions) then directly follows by application of Proposition 6. Since Assumption 1 holds, Proposition 6 implies also that  $\gamma_e, \dot{\gamma}_e, \ddot{x}$  are bounded. Since  $\dot{\gamma}_d(t)$  is bounded, one deduces from (30) that  $\dot{\gamma}_{e,d}(\dot{x}, t)$  remains bounded. Combining with Assumption 4, (29), and Property P1 of the function  $\overline{\text{sat}}_M$ , this implies that  $\dot{\gamma}(\dot{x}, t)$  is also bounded. As a consequence, it follows from (25) that  $u$  and  $\omega_{1,2}$  are well-defined and bounded along each system's solution. This, along with the boundedness of  $\omega_3$ , allows to deduce Property 1 of this theorem.

Let us now establish Property 3. We have that (compare with (9b))

$$\dot{v} = -S(\omega)v - ue_3 + R^T \gamma(\dot{x}, t) + R^T (\gamma_{e,d}(\dot{x}, t) - \overline{\text{sat}}_M(\gamma_{e,d}(\dot{x}, t))) \quad (60)$$

Therefore, the time-derivative of the candidate Lyapunov function  $V$  defined by (12) along the system's solutions is given by

$$\begin{aligned} \dot{V} &= \tilde{v}_3(-u + \bar{\gamma}_3) + \tilde{v}^T R^T (\gamma_{e,d} - \overline{\text{sat}}_M(\gamma_{e,d})) \\ &\quad + \frac{1}{|\gamma|k_2} \begin{pmatrix} \tilde{\gamma}_1 & \tilde{\gamma}_2 \end{pmatrix} \left[ \begin{pmatrix} -\omega_2 \\ \omega_1 \end{pmatrix} + \frac{1}{|\gamma|^2} \begin{pmatrix} -\gamma^T S(Re_2)\dot{\gamma} \\ \gamma^T S(Re_1)\dot{\gamma} \end{pmatrix} + |\gamma|k_2 \begin{pmatrix} \tilde{v}_1 \\ \tilde{v}_2 \end{pmatrix} \right] \end{aligned}$$

Replacing  $u, \omega_1, \omega_2$  by their expressions in (25), one obtains

$$\begin{aligned} \dot{V} &= -|\gamma|k_1\tilde{v}_3^2 - \mu_\tau(|\gamma| + \bar{\gamma}_3) \frac{k_3}{k_2} \frac{\tilde{\gamma}_1^2 + \tilde{\gamma}_2^2}{(|\gamma| + \bar{\gamma}_3)^2} + \tilde{v}^T R^T (\gamma_{e,d} - \overline{\text{sat}}_M(\gamma_{e,d})) \\ &\quad + \frac{(1 - \mu_\tau(|\gamma|))}{|\gamma|^3 k_2} (-\bar{\gamma}_1 \gamma^T S(Re_2)\dot{\gamma} + \bar{\gamma}_2 \gamma^T S(Re_1)\dot{\gamma}) \end{aligned} \quad (61)$$

It follows from (32) and Assumption 4 that

$$\overline{\text{sat}}_M(\gamma_{e,d}(\dot{x}_r(t), t)) = \gamma_{e,d}(\dot{x}_r(t), t)$$

when  $M \geq \bar{c}_1 + \bar{c}_2 \bar{\mathbf{v}}_r^2$ . Using Assumption 2, one deduces that when  $M > \bar{c}_1 + \bar{c}_2 \bar{\mathbf{v}}_r^2$ ,  $\overline{\text{sat}}_M(\gamma_{e,d}(\dot{x}, t)) = \gamma_{e,d}(\dot{x}, t)$  for  $\dot{x}$  in a neighborhood of  $\dot{x}_r$ . Furthermore, since  $\tau \in (0, \delta)$  by assumption one deduces from (24) that  $\mu_\tau(|\gamma|) = 1$  in a neighborhood of  $\dot{x}_r$ . Equation (61) becomes

$$\dot{V} = -|\gamma|k_1\tilde{v}_3^2 - \mu_\tau(|\gamma| + \bar{\gamma}_3) \frac{k_3}{k_2} \frac{\tilde{\gamma}_1^2 + \tilde{\gamma}_2^2}{(|\gamma| + \bar{\gamma}_3)^2}$$

and the proof of local asymptotic stability proceeds like the proof of Proposition 2. Let us now consider the case when  $M \geq \bar{c}_1 + \bar{c}_2(\kappa(\bar{c}_i, \bar{\mathbf{v}}_r))^2$  and  $|\gamma(\dot{x}, t)| \geq \tau, \forall(\dot{x}, t)$ . This latter condition implies that  $\mu_\tau(|\gamma|) = 1, \forall(\dot{x}, t)$ . Therefore, equation (61) becomes

$$\dot{V} = -|\gamma|k_1\tilde{v}_3^2 - \mu_\tau(|\gamma| + \bar{\gamma}_3) \frac{k_3}{k_2} \frac{\tilde{\gamma}_1^2 + \tilde{\gamma}_2^2}{(|\gamma| + \bar{\gamma}_3)^2} + \tilde{v}^T R^T (\gamma_{e,d} - \overline{\text{sat}}_M(\gamma_{e,d}))$$

From Lemma 1 and (61), one deduces that

$$\dot{V} \leq -|\gamma|k_1\tilde{v}_3^2 - \mu_\tau(|\gamma| + \bar{\gamma}_3)\frac{k_3}{k_2}\frac{\bar{\gamma}_1^2 + \bar{\gamma}_2^2}{(|\gamma| + \bar{\gamma}_3)^2}$$

From here, the proof proceeds like the proof of Proposition 2.

## A.8 Lemma 2 and proof

**Lemma 2**

$$\begin{aligned} \frac{d}{dt} \left( \frac{\bar{\gamma}}{|\gamma|} \right) &= \frac{1}{|\gamma|} S(\bar{\gamma}) \left( \omega - \frac{1}{|\gamma|^2} R^T S(\gamma) \dot{\gamma} \right) \\ \frac{d}{dt} \left( 1 - \frac{\bar{\gamma}_3}{|\gamma|} \right) &= \frac{1}{|\gamma|} (\bar{\gamma}_1 \quad \bar{\gamma}_2) \left[ \begin{pmatrix} -\omega_2 \\ \omega_1 \end{pmatrix} + \frac{1}{|\gamma|^2} \begin{pmatrix} -\gamma^T S(Re_2) \dot{\gamma} \\ \gamma^T S(Re_1) \dot{\gamma} \end{pmatrix} \right] \end{aligned}$$

**Proof** Note that  $\frac{\bar{\gamma}}{|\gamma|} = R^T \frac{\gamma}{|\gamma|}$ . Differentiating this equation, one gets

$$\begin{aligned} \frac{d}{dt} \left( \frac{\bar{\gamma}}{|\gamma|} \right) &= -S(\omega) R^T \frac{\gamma}{|\gamma|} + R^T \frac{d}{dt} \left( \frac{\gamma}{|\gamma|} \right) \\ &= -S(\omega) \frac{\bar{\gamma}}{|\gamma|} + R^T \frac{d}{dt} \left( \frac{\gamma}{|\gamma|} \right) \\ &= \frac{1}{|\gamma|} S(\bar{\gamma}) \omega + R^T \frac{d}{dt} \left( \frac{\gamma}{|\gamma|} \right) \end{aligned} \tag{62}$$

Moreover, one has

$$\frac{d}{dt} \left( \frac{\gamma}{|\gamma|} \right) = \frac{(|\gamma|^2 I_3 - \gamma \gamma^T) \dot{\gamma}}{|\gamma|^3} = -\frac{S(\gamma)^2 \dot{\gamma}}{|\gamma|^3}$$

Thus,

$$R^T \frac{d}{dt} \left( \frac{\gamma}{|\gamma|} \right) = -\frac{1}{|\gamma|^3} R^T S(\gamma)^2 \dot{\gamma} = -\frac{1}{|\gamma|^3} S(\bar{\gamma}) R^T S(\gamma) \dot{\gamma} \tag{63}$$

The first result of Lemma 2 is obtained by using (63) in (62). The result is in turn used to obtain

$$\begin{aligned} \frac{d}{dt} \left( 1 - \frac{\bar{\gamma}_3}{|\gamma|} \right) &= -\frac{1}{|\gamma|} e_3^T S(\bar{\gamma}) \left( \omega - \frac{1}{|\gamma|^2} R^T S(\gamma) \dot{\gamma} \right) \\ &= -\frac{1}{|\gamma|} (-\bar{\gamma}_2 \quad \bar{\gamma}_1 \quad 0) \left( \omega - \frac{1}{|\gamma|^2} S(\bar{\gamma}) R^T \dot{\gamma} \right) \\ &= \frac{1}{|\gamma|} (\bar{\gamma}_1 \quad \bar{\gamma}_2) \begin{pmatrix} -\omega_2 \\ \omega_1 \end{pmatrix} + \frac{1}{|\gamma|^3} (\bar{\gamma}_1 \quad \bar{\gamma}_2) \begin{pmatrix} -\gamma^T S(Re_2) \dot{\gamma} \\ \gamma^T S(Re_1) \dot{\gamma} \end{pmatrix} \end{aligned}$$

Note that the variation of  $1 + \frac{\bar{\gamma}_3}{|\gamma|}$  is independent of the yaw angular velocity  $\omega_3$ . ■

### A.9 Barbalat's lemma (see e.g. [18])

**Lemma 3** (*Barbalat*) Let  $x(t)$  denote a solution to the differential equation  $\dot{x} = a(t) + b(t)$  with  $a(t)$  a uniformly continuous function. Assume that  $\lim_{t \rightarrow +\infty} x(t) = c$  and  $\lim_{t \rightarrow +\infty} b(t) = 0$ , with  $c$  a constant value. Then,  $\lim_{t \rightarrow +\infty} \dot{x}(t) = 0$ .

Note that the case  $b = 0$  corresponds to the classical version of Barbalat's lemma.

### A.10 Gain tuning

A way to determine the control gains consists in considering the linearization of System (9) complemented with (17) at the equilibrium ( $z = 0, \dot{z} = 0, \tilde{x} = 0, \tilde{v} = 0, R = I_3, u = g, \omega = 0$ ) for the particular case where the reference trajectory is a fixed point,  $F_e = mge_3$ , and the desired yaw angular velocity is equal to zero. In this appendix, the gain tuning is performed for the position controller of Proposition 5, and the same technique applies to the other controllers.

Near the desired equilibrium,  $\gamma$  as given by (21) can be approximated by

$$\gamma \approx ge_3 + (h(0) + k_z h_z(0))\tilde{x} + h(0)z - 2k_z \dot{z}$$

Setting  $w := \dot{z}$  and using the fact that  $\frac{\partial \sigma(s)}{\partial s}|_{s=0} = 1$ , one deduces from (23) that

$$\begin{cases} u & \approx g + (h(0) + k_z h_z(0))\tilde{x}_3 + gk_1 \tilde{v}_3 + h(0)z_3 + (gk_1 - 2k_z)w_3 \\ \omega_1 & \approx -\frac{k_3}{4g}(h(0) + k_z h_z(0))\tilde{x}_2 - gk_2 \tilde{v}_2 - \frac{k_3 h(0)}{4g}z_2 - (gk_2 - \frac{k_3 k_z}{2g})w_2 - \frac{k_3}{4}(e_2^T R^T e_3) \\ \omega_2 & \approx \frac{k_3}{4g}(h(0) + k_z h_z(0))\tilde{x}_1 + gk_2 \tilde{v}_1 + \frac{k_3 h(0)}{4g}z_1 + (gk_2 - \frac{k_3 k_z}{2g})w_1 + \frac{k_3}{4}(e_1^T R^T e_3) \\ \omega_3 & \approx 0 \end{cases}$$

Define  $\theta_1 := e_1^T R^T e_3$ , and  $\theta_2 := e_2^T R^T e_3$ . It comes from  $\dot{R}^T = -S(\omega)R^T$ ,  $\omega_3 \approx 0$ , and  $R \approx I_3$  that

$$\dot{\theta}_1 \approx -\omega_2, \quad \dot{\theta}_2 \approx \omega_1$$

Using the above approximations, one obtains the following linear system which is the linear approximation of the controlled error system (9) complemented with (17)

$$\begin{cases} \dot{z} & = w \\ \dot{w} & = -2k_z w + k_z h_z(0)\tilde{x} \\ \dot{\tilde{x}} & = \tilde{v} \\ \dot{\tilde{v}} & = (g\theta_1, g\theta_2, -(h(0) + k_z h_z(0))\tilde{x}_3 - gk_1 \tilde{v}_3 - h(0)z_3 - (gk_1 - 2k_z)w_3)^T \\ \dot{\theta}_1 & = -\frac{k_3}{4g}(h(0) + k_z h_z(0))\tilde{x}_1 - gk_2 \tilde{v}_1 - \frac{k_3 h(0)}{4g}z_1 - (gk_2 - \frac{k_3 k_z}{2g})w_1 - \frac{k_3}{4}\theta_1 \\ \dot{\theta}_2 & = -\frac{k_3}{4g}(h(0) + k_z h_z(0))\tilde{x}_2 - gk_2 \tilde{v}_2 - \frac{k_3 h(0)}{4g}z_2 - (gk_2 - \frac{k_3 k_z}{2g})w_2 - \frac{k_3}{4}\theta_2 \end{cases}$$

The preceding system can be decomposed into three independent subsystems

$$\begin{aligned}
 (\bar{\Sigma}_3) : \quad & \begin{cases} \dot{z}_3 = w_3 \\ \dot{w}_3 = -2k_z w_3 + k_z h_z(0) \tilde{x}_3 \\ \dot{\tilde{x}}_3 = \tilde{v}_3 \\ \dot{\tilde{v}}_3 = -(h(0) + k_z h_z(0)) \tilde{x}_3 - g k_1 \tilde{v}_3 - h(0) z_3 - (g k_1 - 2k_z) w_3 \end{cases} \\
 (\bar{\Sigma}_i) : \quad & \begin{cases} \dot{z}_i = w_i \\ \dot{w}_i = -2k_z w_i + k_z h_z(0) \tilde{x}_i \\ \dot{\tilde{x}}_i = \tilde{v}_i \\ \dot{\tilde{v}}_i = g \theta_i \\ \dot{\theta}_i = -\frac{k_3}{4g} (h(0) + k_z h_z(0)) \tilde{x}_i - g k_2 \tilde{v}_i - \frac{k_3 h(0)}{4g} z_i - (g k_2 - \frac{k_3 k_z}{2g}) w_i - \frac{k_3}{4} \theta_i \end{cases} \quad (i = 1, 2)
 \end{aligned}$$

whose characteristic polynomials are given by

$$\begin{aligned}
 P_3(\lambda) &= \lambda^4 + (2k_z + g k_1) \lambda^3 + (h(0) + 2g k_z k_1 + k_z h_z(0)) \lambda^2 \\
 &\quad + (2k_z h(0) + g k_z h_z(0) k_1) \lambda + k_z h_z(0) h(0) \\
 P_i(\lambda) &= \lambda^5 + \left(2k_z + \frac{k_3}{4}\right) \lambda^4 + \left(g^2 k_2 + \frac{k_z k_3}{2}\right) \lambda^3 + \left(2g^2 k_z k_2 + \frac{h(0) k_3}{4} + \frac{k_z h_z(0) k_3}{4}\right) \lambda^2 \\
 &\quad + \left(g^2 k_z h_z(0) k_2 + \frac{k_z h(0) k_3}{2}\right) \lambda + \frac{k_z h_z(0) h(0) k_3}{4}
 \end{aligned}$$

Among many possibilities, one can, for instance, proceed as follows. Take

$$h(0) = 2g k_1 k_z - 4k_z^2, \quad k_2 = \frac{k_1 k_3}{4g}, \quad k_z < \frac{g k_1}{2} \quad (64)$$

Then,

$$\begin{aligned}
 P_3(\lambda) &= (\lambda + 2k_z) \left( \lambda^3 + g k_1 \lambda^2 + (2g k_1 k_z - 4k_z^2 + k_z h_z(0)) \lambda + \frac{1}{2} h_z(0) (2g k_1 k_z - 4k_z^2) \right) \\
 P_i(\lambda) &= (\lambda + 2k_z) \left( \lambda^4 + \frac{k_3}{4} \left( \lambda^3 + g k_1 \lambda^2 + (2g k_1 k_z - 4k_z^2 + k_z h_z(0)) \lambda + \frac{1}{2} h_z(0) (2g k_1 k_z - 4k_z^2) \right) \right)
 \end{aligned}$$

By taking  $2k_z < g k_1$ , one obtains by application of the Routh-Hurwitz criterion that all roots of  $P_3(\lambda)$  have negative real parts. The complementary possibility of having all roots of  $P_3(\lambda)$  real negative and equal leads to choose  $k_1, k_z, h_z(0)$  as follows

$$k_1 = \frac{3\lambda_0}{g}, \quad k_z = \lambda_0, \quad h_z(0) = \lambda_0 \quad (65)$$

with  $\lambda_0$  denoting an arbitrary positive number. Note that  $h(0) = 2\lambda_0^2$  and  $k_2 = \frac{3\lambda_0 k_3}{4g^2}$  in this case. One obtains

$$\begin{aligned}
 P_3(\lambda) &= (\lambda + \lambda_0)^4 \\
 P_i(\lambda) &= (\lambda + \lambda_0) \left( \lambda^4 + \frac{k_3}{4} (\lambda + \lambda_0)^3 \right)
 \end{aligned}$$

Then, it suffices to choose  $k_3$  such that  $k_3 \gg 4\lambda_0$  in order to get the roots of  $P_i(\lambda)$  near those of  $\bar{P}_i(\lambda) := (\lambda + \lambda_0)^3 (\lambda + \frac{k_3}{4})$ . The gains  $k_1, k_2, k_z, h_z(0), h(0)$  used for the simulations of Section 5 have been calculated with  $\lambda_0 = 0.8$  and  $k_3 = 12.8$ .

### A.11 Model of aerodynamic forces and torques

It is assumed that the resultant force  $\vec{F}_{ae}$  of aerodynamic forces applies at a point  $P$  defined by  $\vec{GP} = 0.05\vec{k}$ . Define  $\vec{v}_e := \vec{v}_P - \vec{v}_f$  whose vector of coordinates expressed in the basis of the body-fixed frame  $\mathcal{B}$  is

$$v_e = v_P - v_f = (v + 0.05[\omega_1, \omega_2, 0]^T) - R^T \dot{x}_f$$

Let  $\vec{F}_a$  denote the sum of lift and drag forces,  $\vec{D}_m$  the momentum drag, and  $\vec{F}_{ae} := \vec{F}_a + \vec{D}_m$  the resultant force. With  $F_a$  and  $D_m$  denoting the vector of coordinates of  $\vec{F}_a$  and  $\vec{D}_m$  expressed in the basis of the vehicles's frame  $\mathcal{B}$ , and  $F_{ae}$  the vector of coordinates of  $\vec{F}_{ae}$  expressed in the basis of the inertial frame  $\mathcal{I}$ , one has

$$F_{ae} = R(F_a + D_m)$$

For the simulations we have used

$$\begin{aligned} F_{a,i} &= -k_1^e \sqrt{v_{e,1}^2 + v_{e,2}^2} v_{e,i} - k_2^e |v_e| v_{e,i}, & i = 1, 2 \\ F_{a,3} &= -k_3^e (v_{e,1}^2 + v_{e,2}^2) - k_4^e |v_{e,3}| v_{e,3} \end{aligned}$$

with  $k_1^e = 0.13$ ,  $k_2^e = 0.03$ ,  $k_3^e = 0.03$ ,  $k_4^e = 0.005$ ; and  $D_m = -0.28\sqrt{|T|}v_e$  with  $T$  the thrust force's intensity. The torque induced by the external forces has been calculated according to

$$M_{ae} = -0.05S(e_3)R^T F_{ae}$$



---

Unité de recherche INRIA Sophia Antipolis  
2004, route des Lucioles - BP 93 - 06902 Sophia Antipolis Cedex (France)

Unité de recherche INRIA Futurs : Parc Club Orsay Université - ZAC des Vignes  
4, rue Jacques Monod - 91893 ORSAY Cedex (France)

Unité de recherche INRIA Lorraine : LORIA, Technopôle de Nancy-Brabois - Campus scientifique  
615, rue du Jardin Botanique - BP 101 - 54602 Villers-lès-Nancy Cedex (France)

Unité de recherche INRIA Rennes : IRISA, Campus universitaire de Beaulieu - 35042 Rennes Cedex (France)

Unité de recherche INRIA Rhône-Alpes : 655, avenue de l'Europe - 38334 Montbonnot Saint-Ismier (France)

Unité de recherche INRIA Rocquencourt : Domaine de Voluceau - Rocquencourt - BP 105 - 78153 Le Chesnay Cedex (France)

---

Éditeur  
INRIA - Domaine de Voluceau - Rocquencourt, BP 105 - 78153 Le Chesnay Cedex (France)  
<http://www.inria.fr>  
ISSN 0249-6399